

Mangrove plantation suitability mapping by integrating multi criteria decision making geospatial approach and remote sensing data

Roya Sahraei, Arsalan Ghorbanian, Yousef Kanani-Sadat, Sadegh Jamali & Saeid Homayouni

To cite this article: Roya Sahraei, Arsalan Ghorbanian, Yousef Kanani-Sadat, Sadegh Jamali & Saeid Homayouni (2023): Mangrove plantation suitability mapping by integrating multi criteria decision making geospatial approach and remote sensing data, Geo-spatial Information Science, DOI: [10.1080/10095020.2023.2167615](https://doi.org/10.1080/10095020.2023.2167615)

To link to this article: <https://doi.org/10.1080/10095020.2023.2167615>



© 2023 Wuhan University. Published by Informa UK Limited, trading as Taylor & Francis Group.



Published online: 08 Mar 2023.



Submit your article to this journal [↗](#)



Article views: 189



View related articles [↗](#)



View Crossmark data [↗](#)

Mangrove plantation suitability mapping by integrating multi criteria decision making geospatial approach and remote sensing data

Roya Sahraei ^{a,b}, Arsalan Ghorbanian ^{a,c}, Yousef Kanani-Sadat ^b, Sadegh Jamali ^a
and Saeid Homayouni ^d

^aDepartment of Technology and Society, Faculty of Engineering, Lund University, Lund, Sweden; ^bSchool of Surveying and Geospatial Engineering, College of Engineering, University of Tehran, Tehran, Iran; ^cDepartment of Photogrammetry and Remote Sensing, Faculty of Geodesy and Geomatics Engineering, K. N. Toosi University of Technology, Tehran, Iran; ^dInstitut National de la Recherche Scientifique, Centre Eau Terre Environnement, Québec, Canada

ABSTRACT

Mangroves are woody plant communities that appear in tropical and subtropical regions, mainly in intertidal zones along the coastlines. Despite their considerable benefits to humans and the surrounding environment, their existence is threatened by anthropogenic activities and natural drivers. Accordingly, it is vital to conduct efficient efforts to increase mangrove plantations by identifying suitable locations. These efforts are required to support conservation and plantation practices and lower the mortality rate of seedlings. Therefore, identifying ecologically potential areas for plantation practices is mandatory to ensure a higher success rate. This study aimed to identify suitable locations for mangrove plantations along the southern coastal frontiers of Hormozgan, Iran. To this end, we applied a hybrid Fuzzy-DEMATEL-ANP (FDANP) model as a Multi-Criteria Decision Making (MCDM) approach to determine the relative importance of different criteria, combined with geospatial and remote sensing data. In this regard, ten relevant sources of environmental criteria, including meteorological, topographical, and geomorphological, were used in the modeling. The statistical evaluation demonstrated the high potential of the developed approach for suitable location identification. Based on the final results, 6.10% and 20.80% of the study area were classified as very-high suitable and very-low suitable areas. The obtained values can elucidate the path for decision-makers and managers for better conservation and plantation planning. Moreover, the utility of charge-free remote sensing data allows cost-effective implementation of such an approach for other regions by interested researchers and governing organizations.

ARTICLE HISTORY

Received 18 April 2022
Accepted 9 January 2023

KEYWORDS

Mangrove; remote sensing; geospatial analysis; Fuzzy-DEMATEL-ANP; plantation allocation; analytic hierarchy process (AHP); multi criteria decision making (MCDM)

1. Introduction

Mangroves are a community of woody plants which grow in tropical and subtropical regions, mainly along coastlines and intertidal areas (Syahid et al. 2020; Sakti et al. 2020). Structure-wise, they are a combination of tree and shrub species that can flourish under harsh environmental conditions such as high salinity and high temperature (Osei Darko et al. 2021). Mangroves provide essential benefits to humans and their surrounding environments in many ways, such as reducing the impact of shoreline erosion and storms (Maurya, Mahajan, and Chaube 2021), acting as water purifiers (Hu et al. 2020), being a source of income, food, fuel, and medicine (Melo et al. 2020) and providing habitat for many species (Syahid et al. 2020). More particularly, by sequestering 1.023 Mg per hectare of carbon, they play a crucial role in carbon sequestration and mitigating climate change (Veettil et al. 2020; Syahid et al. 2020; Omar, Misman, and Musa 2019).

Despite mangroves' advantages, their survival has been threatened by anthropogenic activities and natural drivers (Omo-Irabor et al. 2011; DATTA and

DEB 2012). Regarding the human-induced activities, mangroves are mostly eradicated for fuel (Mark et al. 2017), and their corresponding areas are transited to other land uses such as rice fields, aquacultures, and fisheries (Cormier-Salem and Panfili 2016). Moreover, climate change, sea-level rise, natural hazards, and ecological anomalies are among the natural drivers of mangroves' loss (Woodroffe 1990; Syahid et al. 2020). Approximately 20–30% of mangroves all around the world have faded away over the last 50 years (Giri 2021), and the situation is getting worse by the end of 21 century, especially in Asia, which has a 40% share of the world's mangroves (Veettil et al. 2020).

Mangrove communities have been recognized as a beneficial component of the United Nations Sustainable Development Goals (UN-SDGs) (Swamy et al. 2018). Therefore, mapping and monitoring their state in spatial and temporal manners are vital for sustainable management (Ghosh, Kumar, and Roy 2016). More particularly, identifying suitable locations for planting mangroves and having a strategic plan for their conservation are obligatory to increase and save them worldwide (Hu et al. 2020). In this way, it is

essential to undertake effective workflows to identify ecologically suitable locations for mangrove plantations (Hu et al. 2020). The suitability allocation allows for achieving higher success rates in mangrove plantation practices and lowers the mortality rates in the mangrove seedlings. Various ecological criteria, such as climatic criteria, geomorphic parameters, flora conditions, and human interfaces, should be incorporated to support exhaustive suitability mapping (Chakraborty et al. 2019). Most of these factors are available through Remote Sensing (RS) and have been effectively employed in mangroves studies with different purposes (Veettil et al. 2020; Dahdouh-Guebas 2002). Compared to field-based methods, RS provides frequent datasets with consistent spatial coverage permitting investigations over large-scale areas (Kamal, Phinn, and Johansen 2015; Baloloy et al. 2020; Ghorbanian et al. 2022; dela Torre et al. 2021).

Furthermore, it is possible to integrate and manipulate various RS datasets within Geographic Information System (GIS) environments (Al-Hanbali et al. 2021). Many studies have employed the combination of RS and GIS for mangrove investigations (Jumawan and Macandog 2021; Jayanthi et al. 2018; Pattanaik and Prasad 2011). For instance, a study in Southeast Asia utilized a combined GIS and RS technique to determine the mangrove loss drivers in Southeast Asia by identifying the foremost land covers that substituted deforested mangroves between 2000 and 2012 (Richards and Friess 2016). Likewise, Maurya, Mahajan, and Chaube (2021) stated that the combination of satellite data acquired by RS and the GIS environment is the most practical and handiest way for mangrove ecosystem monitoring. Furthermore, Sushobhan et al. (2022) implemented an object-based modeling approach using four Normalized Difference Vegetation Index (NDVI) images with ten years interval to examine mangrove dynamics in Sundarbans, India. They reported a high mangrove disappearance due to sea-level rise, anthropogenic activities, and a lack of conservation policies.

The flexibility of GIS allows combining different criteria through the Multi-Criteria Decision Making (MCDM) methods. One of the well-known MCDM methods is the Analytic Hierarchy Process (AHP), widely used in natural hazards and spatial modeling studies (Das 2020). The AHP method provides the relative importance of considered criteria (i.e. weights), and the final spatial modeling map (i.e. suitability or risk) is generated through the Weighted Linear Combination (WLC) procedure (Shabani, Masoumi, and Rezaei 2022). In recent years, the AHP method has also been implemented in a few mangrove studies to weight the considered mangroves restoration and plantation allocation criteria. Scholars declared that this group of methods had shown satisfactory results (Chakraborty et al. 2019; Matani et al.

2021). In another study, over the last 20 years, RS datasets were employed to identify the different criteria for the degradation of mangrove forests using the Delphi technique. The AHP method was then implemented to rank and weight these criteria for remediality and preventability. The authors declared that the result of their study could aid policymakers in having an insight into mangrove ecosystem management and sustainability (Savari, Damaneh, and Damaneh 2022).

Despite the popularity and convenience of the AHP method, it includes a few limitations that require further consideration. One of these limitations is that experts state their opinions using crisp numbers, leading to bias or inconsistency (Chen et al. 2011). Also, the involved criteria in allocation studies (e.g. mangrove plantation suitability) probably are correlated considering their geographical aspect. Consequently, they could have different levels of reciprocal impacts, which should be considered (Arabsheibani, Kanani Sadat, and Abedini 2016; Kanani-Sadat et al. 2019). Therefore, to overcome the mentioned shortcomings that have been precluded in previous mangrove plantation studies, we applied a hybrid MCDM method. In this hybrid approach, DEcision-MAking Trial and Evaluation Laboratory (DEMATEL) method was integrated with fuzzy logic, and then the results were incorporated into the Analytical Network Process (ANP) method as an improved version of AHP. Fuzzy logic is a solution to handle the uncertainty of using crisp numbers by utilizing fuzzy membership functions, eliminating or decreasing the corresponding vagueness (Feizizadeh et al. 2014). Also, DEMATEL is an efficient approach for investigating and identifying the interconnection between criteria involved in a complicated problem (Büyüközkan and Çifçi 2012). The efficiency of the DEMATEL method for dealing with interdependencies between criteria has been stated in many studies that could ensure achieving more reliable results (Wang et al. 2019).

Accordingly, this paper aims to (1) identify ecologically suitable areas for mangrove plantation by incorporating ten criteria in different categories (i.e. topographical, geomorphological, and meteorological) in Hormozgan province, southern Iran, (2) investigate the efficiency of the Fuzzy-DEMATEL approach combined with the ANP method for the criteria weighting task, and (3) examine the performance of Fuzzy-DEMATEL-ANP (FDANP) approach over the conventional AHP approaches that were employed in previous mangrove plantation allocation studies. In this regard, ten relevant sources of environmental criteria, such as (1) precipitation, (2) elevation, (3) slope, (4) wind, (5) temperature, (6) solar radiation, (7) NDVI, (8) Normalized Difference Salinity Index (NDSI), (9) Normalized Difference Moisture Index (NDMI), and (10) Land Use and Land Cover (LULC) were incorporated to generate mangrove

plantation suitability map. Finally, visual comparisons and statistical evaluations were performed to examine the suitability of the implemented approach.

2. Study area

Mangroves exist along the Persian Gulf and Oman Sea coastal areas in three southern provinces of Iran. The study area of this research is the entire coastal area of Hormozgan province, which is home to the Hara Protected Area, the largest mangrove ecosystem in the Persian Gulf and Oman Sea. The study area lies between 25° 24' and 28° 57' latitudes and 53° 41' and 59° 15' longitudes and covers an area of over 7000 km² (see Figure 1). The border length of the study area, as the coastal boundary of Hormozgan province, facing the Persian Gulf and Oman Sea, is approximately 900 km. The mean annual temperature in this region varies between 21.5°C and 53.7°C. The study area hosted two types of mangroves, namely *Avicennia marina* and *Rhizophora mucro*, with the dominant portion of the former (Ghorbanian et al. 2021), which have been recognized as excellent sources of carbon sink (Amiri 2021; El Hussieny, Shaltout, and Alatar 2021). Except for the Hara Protected area, the study area inhabits several other mangrove ecosystems patches (Mafi-Gholami et al. 2020; Alireza and Beglu Mansour 2012) and is thus considered one of the potentially suitable areas for mangrove plantations.

3. Material and methods

3.1. Datasets

3.1.1. Remote sensing and geospatial data

For mangrove suitability mapping, ten environmental factors and geospatial layers of criteria from different categories (i.e. topographical, geomorphological, and meteorological) were considered. These criteria were

chosen based on the previous literature that incorporated relevant criteria for mangrove plantation allocation or the proven fact of their impact on mangrove health and data availability over the study area (Chakraborty et al. 2019; Savari, Damaneh, and Damaneh 2022). Consequently, ten criteria of (1) precipitation, (2) elevation, (3) slope, (4) wind, (5) temperature, (6) solar radiation, (7) NDVI, (8) NDSI, (9) NDMI, and (10) LULC were employed. These datasets were collected and analyzed using the cloud computing platform of Google Earth Engine (GEE). This cloud computing platform allows the visualization, prototyping, and processing of many open-access RS and geospatial datasets (Ravanelli et al. 2018; Gorelick et al. 2017; Amani et al. 2020). GEE hosts multi-petabyte satellite imagery and geospatial catalogs, making it an appealing choice for large-scale and multi-criteria data preparation and manipulation. Given that this information was acquired/generated from different sources, either downscaling or upscaling step was applied to the original datasets to make all consistent in terms of spatial resolution (i.e. 100 m) for further processing.

Afterward, all the involved criteria were normalized in a GIS environment for criteria range compatibility. In particular, if the higher value of a criterion was associated with higher mangrove suitability, it was normalized by $y = \frac{x - x_{min}}{x_{max} - x_{min}}$ (direct), otherwise $y = \frac{x_{max} - x}{x_{max} - x_{min}}$ (inverse) was used, where x and y are the un-normalized and normalized values of each criterion, respectively. x_{min} and x_{max} are respectively the lowest and highest value of each layer. NDVI, NDMI, solar radiation, and precipitation were normalized using the former equation (direct). Also, wind and slope were normalized using the latter equation (inverse) because they impact mangrove suitability contrariwise. Furthermore, according to temperature data in the

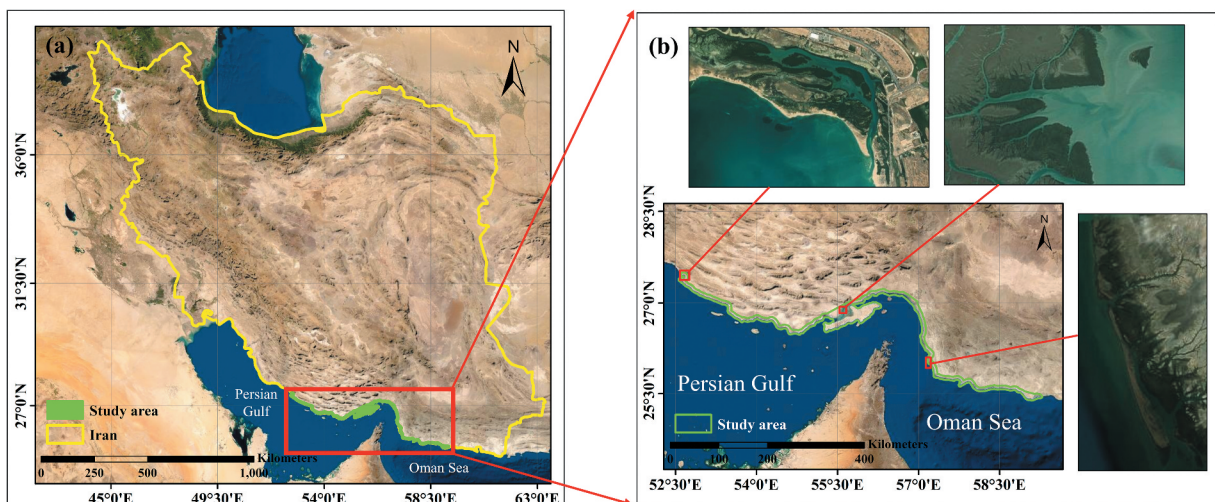


Figure 1. (a) Geographical location of the study area in the southern part of the country extending along the Persian Gulf and Oman Sea; (b) study area along with four zoomed patches of very high-resolution images for better representation.

study area, we split the values of this criterion into two groups. The earlier direct equation normalized those areas with a temperature less than 34°C, and areas with higher temperatures were normalized by the inverse equation.

Moreover, the elevation values lower than 4 m were normalized using the direct equation, and otherwise, an inverse equation was used. The normalization of the LULC criterion was different from other criteria, which were applied based on experts' knowledge, and a pair-wise comparison was considered to evaluate the suitability of different classes in the GIS environment. The criteria summary is provided in Table 1, and the final prepared criteria are presented in Figure 2.

3.1.2. Reference data

In addition to satellite and geospatial datasets, reference data in two classes of mangrove and non-mangrove were collected spreading over the study area. These samples were collected through precise visual inspection of very-high-resolution satellite

imagery available within ArcMap and Google Earth. A total of 1015 reference samples for mangrove classes and 1015 reference samples for non-mangrove classes were selected. The reference samples were employed to fulfill two tasks (1) retrieving point values of different criteria for the mangrove class to support a better weighting procedure and (2) applying statistical evaluation to ensure the reliability of the implemented approach.

3.2. Methodology

This section covers the methodological aspects of producing a mangrove plantation suitability map. Figure 3 presents the workflow of the implemented approaches to integrate different criteria for mangrove plantation allocation. In this regard, the Pearson correlation coefficient values between the considered criteria are calculated to examine the possible interdependencies among them. Then, the developed FDANP method is thoroughly described, followed by

Table 1. Summary of sources and data preparation descriptions of all considered mangrove plantation suitability mapping criteria.

NO.	Criterion	Source	Description	Reference
1	Precipitation	Climate Hazards Group InfraRed Precipitation with Station data (CHIRPS)	The study area's daily accumulated precipitation data were used to calculate this criterion. The time duration was between January and July 2020. The original data had a 5566 m spatial resolution that was resampled to 100 m using the nearest neighbor method.	(Funk et al. 2015)
2	Elevation	Shuttle Radar Topography Mission (SRTM)	This topographic criterion was generated at a 100 m spatial resolution using the SRTM Digital Elevation Data Version 4. The original data had a 90 m spatial resolution that was resampled to 100 m using the nearest neighbor method.	(Jarvis et al. 2008)
3	Slope	Elevation (SRTM)	This topographic criterion was calculated using the SRTM Digital Elevation Data Version 4 dataset. The original data had a 90 m spatial resolution that was resampled to 100 m using the nearest neighbor method.	(Jarvis et al. 2008)
4	Wind	Global Forecast System (GFS)	The wind criterion consisted of two components, including v_component and u_component of wind. We aggregated these two components in the GIS environment to create the wind layer using this formula: $\sqrt{(v_component)^2 + (u_component)^2}$ The original data had a 27,830 m spatial resolution that was resampled to 100 m using the nearest neighbor method.	(Alpert 2004)
5	Temperature	Landsat-8	The mean temperature was considered for the study area between January and July 2020. The original data had a 30 m spatial resolution that was resampled to 100 m using the nearest neighbor method.	USGS
6	Solar radiation	National Centers for Environmental Prediction (NCEP) Climate Forecast System	The mean value of solar radiation for the study area was considered between January and July 2020. The original data had a 22,264 m spatial resolution that was resampled to 100 m using the nearest neighbor method.	(Saha et al. 2011)
7	NDVI	Landsat-8	NDVI is an indicator that evaluates the condition of healthy green vegetation using near-infrared (NIR) and Red spectra of Landsat 8. It was calculated using $NDVI = \frac{NIR - R}{NIR + R}$ The mean value for a one-year duration (January 2020- January 2021) was considered. The original data had a 30m spatial resolution that was resampled to 100 m using the nearest neighbor method.	USGS
8	NDSI	Landsat-8	The NDSI index uses NIR and Red bands to provide a proxy for the salinity condition of the salt-affected area and was calculated by. The mean value for a one-year duration (January 2020- January 2021) was considered.	USGS
9	NDMI	Landsat-8	The normalized difference moisture index (NDMI) was derived from the NIR and the SWIR band using $NDMI = \frac{NIR(4) - SWIR(5)}{NIR(4) + SWIR(5)}$ The mean value for a one-year duration (January 2020- January 2021) was considered.	USGS
10	LULC	Copernicus Global Land Cover (CGLC)	The LULC map of the study area had seven classes after reclassification of the original map obtained from GEE. The following classes are included in this criterion: unknown and bare, woody vegetation, agriculture and vegetation, urban, forest, waterbody, and wetlands. The original data had a 100m spatial resolution.	(Buchhorn et al. 2020)

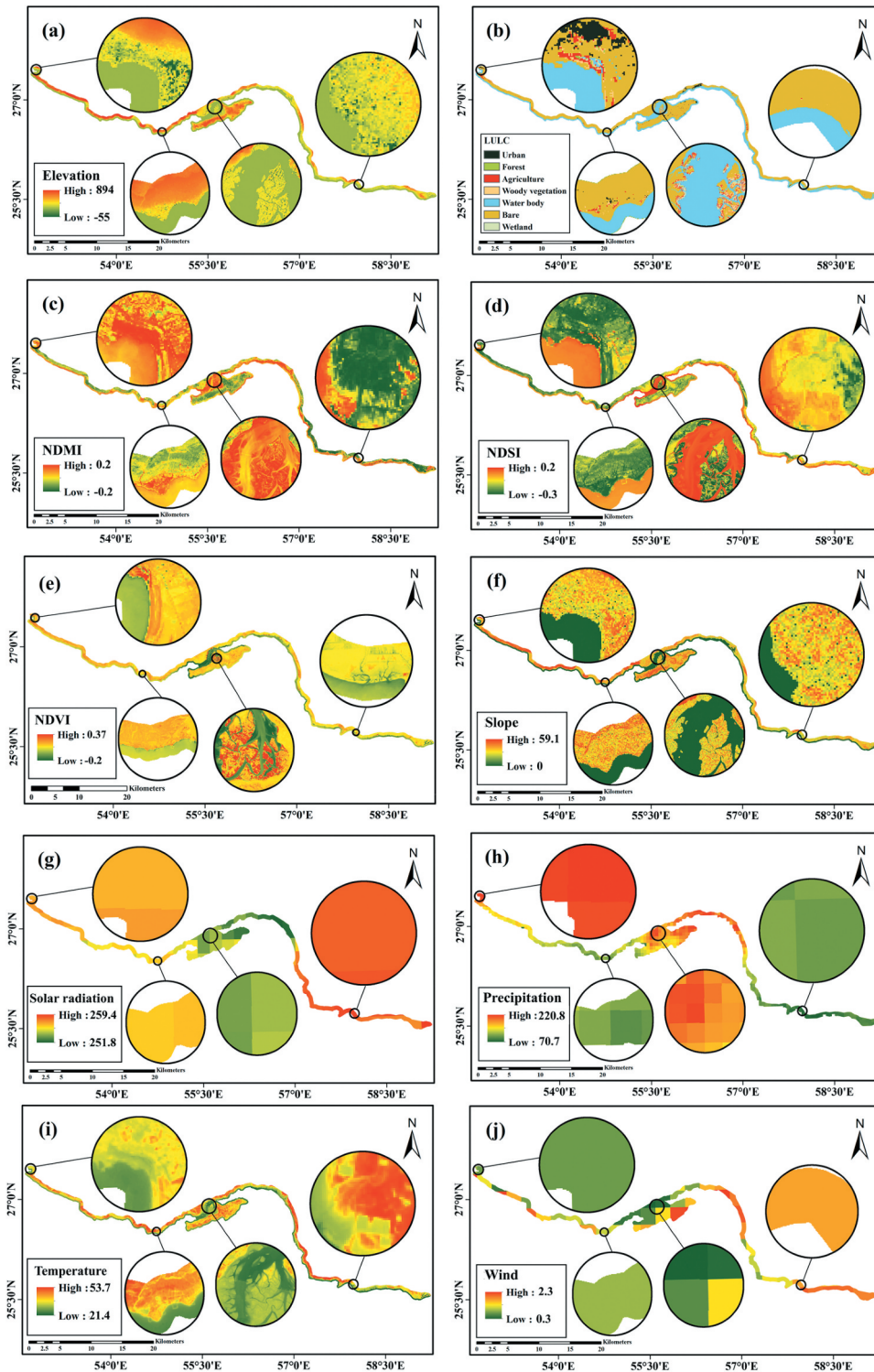


Figure 2. The spatial variability of (a) elevation, (b) LULC, (c) NDMI, (d) NDSI, (e) NDVI, (f) Slope, (g) solar radiation, (h) precipitation, (i) temperature, (j) wind across the study area.

a brief explanation of the conventional AHP method, which has been adopted in previous mangrove studies (Savari, Damaneh, and Damaneh 2022; Syahid et al. 2020; Jumawan and Macandog 2021). Finally, the validation procedure using collected reference samples for quality assurance is described.

3.2.1. Fuzzy-DEMATEL-ANP (FDNAP) algorithm

FDNAP is a hybrid MCDM method that incorporates the fuzzy logic and interrelationships of considered criteria to improve the final results compared to more conventional MCDM methods (Phochanikorn and Tan 2019). In complex decision-making

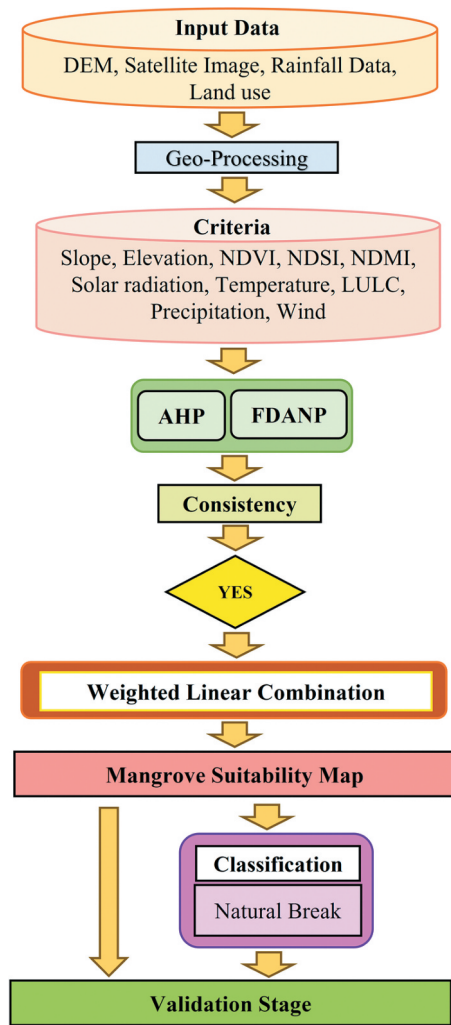


Figure 3. Flowchart of the proposed methodology for mangrove plantation suitability mapping.

problems, directly/indirectly interdependent criteria with reciprocal impacts exist. Accordingly, to ensure an improved MCDM, it must sufficiently detect mutual interactions and turn them into an understandable model for further processing. One method is the DEMATEL (Gabus and Fontela 1973), which takes the “Cause” and “Effect” interactions between input criteria using graphs and matrices (Falatoonitoosi, Ahmed, and Sorooshian 2014). DEMATEL has proven to be an effective procedure for examining and considering the reciprocal interactions between different criteria (Sorourkhah and Edalatpanah 2022). Accordingly, since the objective of the current study is to identify ecologically suitable areas for mangrove plantation by considering ten criteria, which may have possible interrelationships, the DEMATEL method was considered. A sample of the DEMATEL diagram and matrix is shown in Figure 4, in which the numbers 0, 1, 2, 3, and 4 depict “no influence”, “very low influence”, “low influence”, “high influence”, and “very high influence”, respectively. As an example, in Figure 4, it can be seen that C4 has a major impact on C3, though it has less impact on C5.

The relative importance and preferences of considered criteria are provided based on one’s acquaintance and experience. They are declared using linguistic values, which as a human-centered operation, definitely includes uncertainty. Accordingly, it is suggested to incorporate linguistics variables from fuzzy logic instead of crisp numbers as the relative importance of all criteria (Kanani-Sadat et al. 2019; Soner

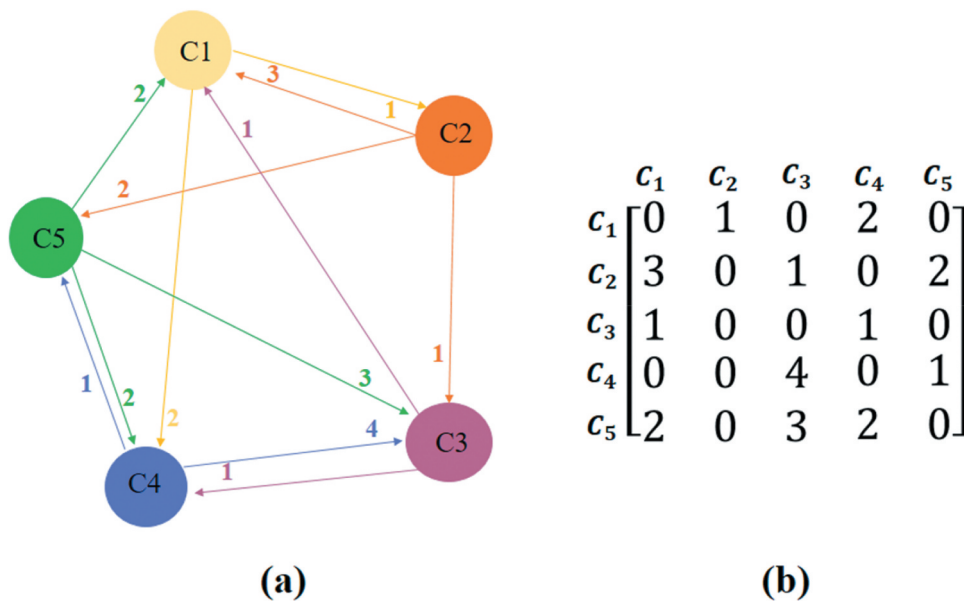


Figure 4. (a) the direct graph and (b) matrix form of a schematic sample of a typical causal relationship between five arbitrary criteria.

2021). Therefore, to implement a trustworthy MCDM framework, the vagueness in the verbal terms has to be reduced or even eliminated (Gigović et al. 2016; Sangaiah et al. 2017; Ayçin and Kayapinar Kaya 2021). In order to handle the inherent uncertainty and ambiguity in one's opinion, fuzzy variables introduced by (Zadeh, Klir, and Yuan 1996) can be utilized. Therefore, we combined fuzzy logic with the DEMATEL method to explore the causal relationships between criteria and build a network-based structure with the ANP method. Consequently, the final weight values of all criteria are calculated, and then they are integrated through a WLC method to generate the suitability map. In this hybrid approach, the following six steps are required to calculate weight values.

- **Step 1: Fuzzy direct relation matrix**

In this step, k number of pair-wise comparison matrices containing the reciprocal influence criteria in verbal terms format are collected. Later, Fuzzy Triangular Membership Functions (FTMF) are defined as $E_{ij}^k = (l_{ij}^k, m_{ij}^k, u_{ij}^k)$, where E_{ij}^k is the judgment regarding the impact of i^{th} criterion on j^{th} criterion made by k^{th} expert. Fuzzy lingual expressions and the corresponding FTMF specifications are provided in Table 2. Afterward, the fuzzy direct relation matrix (\tilde{A}) is computed using Equation (1), in which \tilde{A} is the fuzzy direct-relation and N indicates the number of experts.

$$\tilde{A} = \frac{(\tilde{E}^1 \oplus \tilde{E}^2 \oplus \dots \oplus \tilde{E}^N)}{N} \quad (1)$$

below, the structure of \tilde{A} is shown.

$$\tilde{A} = \begin{bmatrix} 0 & \tilde{a}_{12} & \dots & \tilde{a}_{1n} \\ \tilde{a}_{21} & 0 & \dots & \tilde{a}_{2n} \\ \vdots & \vdots & \ddots & \vdots \\ \tilde{a}_{n1} & \tilde{a}_{n2} & \dots & 0 \end{bmatrix} \quad (2)$$

- **Step 2: Normalizing the fuzzy direct relation matrix**

The normalized fuzzy direct relation matrix (\tilde{X}) is generated by applying Equation (3) to the \tilde{A} (Mavi and Standing 2018).

$$x_{ij} = \frac{a_{ij}}{s} = \left(\frac{l_{ij}}{s}, \frac{m_{ij}}{s}, \frac{u_{ij}}{s} \right), s = \max \left[\max_{1 \leq i \leq n} \left(\sum_{j=1}^n u_{ij} \right), \max_{1 \leq j \leq n} \left(\sum_{i=1}^n u_{ij} \right) \right] \quad (3)$$

below, the structure of \tilde{X} is shown.

$$\tilde{X} = \begin{bmatrix} 0 & \tilde{x}_{12} & \dots & \tilde{x}_{1n} \\ \tilde{x}_{21} & 0 & \dots & \tilde{x}_{2n} \\ \vdots & \vdots & \ddots & \vdots \\ \tilde{x}_{n1} & \tilde{x}_{n2} & \dots & 0 \end{bmatrix} \quad (4)$$

- **Step 3: Acquiring the fuzzy total relation matrix**

In this stage, the fuzzy total relation matrix (\tilde{T}) that includes both direct and indirect interactions between all criteria is generated using Equations (5)–(6).

$$\tilde{T} = \begin{bmatrix} \tilde{t}_{11} & \tilde{t}_{12} & \dots & \tilde{t}_{1n} \\ \tilde{t}_{21} & \tilde{t}_{22} & \dots & \tilde{t}_{2n} \\ \vdots & \vdots & \ddots & \vdots \\ \tilde{t}_{n1} & \tilde{t}_{n2} & \dots & \tilde{t}_{nn} \end{bmatrix}, \tilde{t}_{ij} = (l_{ij}'' , m_{ij}'' , u_{ij}'') , \quad i, j = 1, 2, \dots, n \quad (5)$$

$$\begin{aligned} [l_{ij}''] &= X_l \times (I - X_l^{-1}), [m_{ij}''] \\ &= X_m \times (I - X_m^{-1}), [u_{ij}''] = X_u \times (I - X_u^{-1}) \end{aligned} \quad (6)$$

later, the fuzzy total relation matrix (\tilde{T}) is defuzzified using Equation 7 to ease the comprehension of the mutual impacts of criteria and provide a better insight into the relations and interactions among criteria. It is worth noting that during the defuzzification step of the fuzzy total relation matrix, elements with negligible values (low reciprocal influence) are filtered out (i.e. set to 0) using the α -cut threshold defined by experts (Vinodh, Sai Balagi, and Patil 2016; Kanani-Sadat et al. 2019). The α -cut total-relation matrix total-relation matrix (T_α) is shown in Equation 8.

$$T_{ij}^{def} = \frac{l_{ij}'' + 4m_{ij}'' + u_{ij}''}{6} \quad (7)$$

$$T_\alpha = \begin{bmatrix} t_{11}^\alpha & t_{12}^\alpha & \dots & t_{1n}^\alpha \\ t_{21}^\alpha & t_{22}^\alpha & \dots & t_{2n}^\alpha \\ \vdots & \vdots & \ddots & \vdots \\ t_{n1}^\alpha & t_{n2}^\alpha & \dots & t_{nn}^\alpha \end{bmatrix} \quad (8)$$

- **Step 4: Calculate the fuzzy values of D and R**

The summation of i^{th} row (see Equation (9)) of the \tilde{T} gives the \tilde{R} values as the indicator of the direct/indirect impact of criterion i^{th} on others (Jassbi, Mohamadnejad, and Nasrollahzadeh 2011). Moreover, \tilde{D}_j indicates the overall impacts of all

Table 2. The implemented fuzzy triangular membership functions (FTMF) versus verbal terms.

Lingual term	Influence level				
	No	Very low	low	High	Very high
FTMF numbers	(0, 0, 0.25)	(0, 0.25, 0.5)	(0.25, 0.5, 0.75)	(0.5, 0.75, 1.0)	(0.75, 1.0, 1.0)

criteria on the j^{th} criterion that is calculated by summing the j^{th} column (see Equation (10)) of the \tilde{T} (Jassbi, Mohamadnejad, and Nasrollahzadeh 2011).

$$\tilde{R} = [\tilde{R}_i]_{n \times 1} = \sum_{j=1}^n \tilde{t}_{ij} \quad (9)$$

$$\tilde{D} = [\tilde{D}_j]_{1 \times n} = \sum_{i=1}^n \tilde{t}_{ij} \quad (10)$$

- **Step 5: Defuzzification of $\tilde{R}_i + \tilde{D}_i$ and $\tilde{R}_i - \tilde{D}_i$ values**

In order to acquire the casual relations between all criteria and calculate their importance, $\tilde{R}_i + \tilde{D}_j$ and $\tilde{R}_i - \tilde{D}_j$ are defuzzified based on Equation (11). In this way, the strength of the impact of the i^{th} criterion on the other criteria is evaluated by $\tilde{R}_i + \tilde{D}_i$. Meanwhile, the positive value of $\tilde{R}_i - \tilde{D}_j$ is a sign of the effectiveness of i^{th} criterion and settles into the ‘‘Causes’’ group. Moreover, the i^{th} criterion, which takes influence from others, settles into the group of ‘‘Effects’’ in the case that $\tilde{R}_i - \tilde{D}_j$ value is negative. Criterion with a higher $\tilde{R}_i - \tilde{D}_j$ value has a considerable impact on others and has a higher priority; consequently, criteria that have lower values of $\tilde{R}_i - \tilde{D}_j$ are those affected by other criteria, hence, have a lower priority (Jassbi, Mohamadnejad, and Nasrollahzadeh 2011; Kanani-Sadat et al. 2019).

$$(\tilde{R} \pm \tilde{D})^{def} = \frac{(\tilde{R} \pm \tilde{D})_l^{fuzzy} + 4(\tilde{R} \pm \tilde{D})_m^{fuzzy} + (\tilde{R} \pm \tilde{D})_u^{fuzzy}}{6} \quad (11)$$

- **Step 6: Calculating the criteria weights through ANP**

In the final step, the weight value of each criterion is calculated based on the ANP method that considers the interdependencies among factors (Saaty 1996). In the ANP method, hierarchical structure restriction is eliminated, and a network model is used efficiently to manage the interdependencies between the criteria. Therefore, applying the ANP approach can lead to more satisfactory results with interdependent relationships (Ghorbanzadeh, Feizizadeh, and Blaschke 2018). To this end, the relative importance pair-wise comparison matrix is generated based on crisp numbers between 1 to 9, with higher importance by increasing the value (Saaty 1996). Equation (12) shows the general form of the super-matrix in which C_n refers to the n^{th} criterion, and W_{ij} points to the effect of j^{th} criterion on the objective compared with the i^{th} criterion.

$$W = \begin{matrix} & C1 & C2 & \dots & Cn \\ \begin{matrix} C1 \\ C2 \\ \vdots \\ Cn \end{matrix} & \begin{bmatrix} W_{11} & W_{12} & \dots & W_{1n} \\ W_{21} & W_{22} & \dots & W_{2n} \\ \vdots & \vdots & \ddots & \vdots \\ W_{n1} & W_{n2} & \dots & W_{nn} \end{bmatrix} \end{matrix} \quad (12)$$

later, a weighted pair-wise comparison matrix (W_w) is generated by multiplying the normalized α -cut total relation matrix (T_s) (see Equation (13)) by the relative importance pair-wise comparison matrix (W), and the results are called a weighted super-matrix (W_w in Equation (14)). Finally, by limiting W_w powered to a large enough number (Equation (15)), the weighted super-matrix W_w converges to a long-term stable matrix. Consequently, each element in each row renders the conclusive weights of the criteria (Ali et al. 2020).

$$T_s = \begin{bmatrix} \frac{t_{11}^\alpha}{d_1} & \frac{t_{12}^\alpha}{d_1} & \dots & \frac{t_{1n}^\alpha}{d_1} \\ \frac{t_{21}^\alpha}{d_2} & \frac{t_{22}^\alpha}{d_2} & \dots & \frac{t_{2n}^\alpha}{d_2} \\ \vdots & \vdots & \ddots & \vdots \\ \frac{t_{n1}^\alpha}{d_n} & \frac{t_{n2}^\alpha}{d_n} & \dots & \frac{t_{nn}^\alpha}{d_n} \end{bmatrix} = \begin{bmatrix} t_{11}^s & t_{1j}^s & \dots & t_{1n}^s \\ t_{i1}^s & t_{ij}^s & \dots & t_{in}^s \\ \vdots & \vdots & \ddots & \vdots \\ t_{n1}^s & t_{nj}^s & \dots & t_{nn}^s \end{bmatrix} d_i = \sum_{j=1}^n t^{\alpha} ij \quad (13)$$

$$W_w = \begin{bmatrix} t_{11}^s \times W_{11} & \dots & t_{1i}^s \times W_{j1} & \dots & t_{1n}^s \times W_{n1} \\ \vdots & \ddots & \vdots & \ddots & \vdots \\ t_{i1}^s \times W_{1i} & \dots & t_{ij}^s \times W_{ji} & \dots & t_{in}^s \times W_{ni} \\ \vdots & \vdots & \vdots & \ddots & \vdots \\ t_{n1}^s \times W_{1n} & \dots & t_{nj}^s \times W_{jn} & \dots & t_{nn}^s \times W_{nn} \end{bmatrix} \quad (14)$$

$$W_L = \lim_{p \rightarrow \infty} (W_w)^p \quad (15)$$

3.2.2. Analytical hierarchy process algorithm

AHP is an MCDM approach that includes organizing different criteria into a hierarchy, determining their relevant importance, comparing alternative solutions for each criterion, and deciding the final ranking based on suitability, risk, and cost (Saaty 1977, 1980; Feloni, Mousadis, and Baltas 2020). The first step of the AHP is determining the relative importance of each criterion regarding other criteria for suitability mapping. In this regard, the relative importance values are determined by numerical values, ranging between 1 and 9, with higher importance by increasing the value (Mahmoud and Gan 2018), leading to a pair-wise matrix. According to the number of generated pair-wise matrices, it might be required to calculate the average pair-wise matrix using the geometric mean using Equation (16)

$$A_{ave} = \sqrt[k]{\prod_{i=1}^k A_i} \quad (16)$$

where k is the number of experts, A_i is the pair-wise matrix of i^{th} expert, and A_{ave} is the average pair-wise matrix. The next step is to normalize the final pair-wise matrix by dividing each column element by the corresponding column's sum using Equation (17)

$$a_{ij}' = \frac{a_{ij}}{\sum_{i=1}^n a_{ij}} \quad (17)$$

where n is the number of criteria, a_{ij} is the value of the criterion in the pair-wise matrix, and a_{ij}' is the normalized criterion (Cabrera and Lee 2020).

Later, the final weight value of each criterion is calculated by summing the elements of each row and dividing them by order of the matrix using Equation (18) (Bouamrane et al. 2020).

$$W_i = \frac{\sum_{j=1}^N a_{ij}'}{N} \quad (18)$$

where N represents the order of the matrix (Bouamrane et al. 2020).

Afterward, the Consistency Ratio (CR) was calculated to ensure the correctness and suitability of the weight value determination step (see Equation (19)). In this regard, first, the Consistency Index (CI) must be calculated, and the Random Inconsistency (RI) was set at 1.49 (Saaty 1980; Dano 2021). CR values less than 0.1 indicate a suitable pair-wise matrix; otherwise, the pair-wise matrix should be reconsidered. All criteria are integrated through the WLC method to generate the suitability maps using weights obtained by implemented methods in this study at the final step using Equation (20)

$$CR = \frac{CI}{RI}, CI = \frac{\lambda_{max} - n}{n - 1} \quad (19)$$

$$MSM = \sum_{i=1}^n W_i \times C_i \quad (20)$$

3.2.3. Accuracy assessment

Accuracy assessment is an essential step to ensure the reliability of the produced suitability map. Accordingly, several statistical parameters were calculated to validate the final suitability results. It is worth noting that the collected reference samples were employed for accuracy assessment. First, the Receiver Operator Characteristics (ROC), as a broadly used approach to determine the capability of spatial modeling, was applied (Chen et al. 2011; Samanta et al. 2018; Falah et al. 2019). To this end, the ROC curve was plotted in 2D space for different threshold values, which displayed the model's sensitivity and specificity (see Equations (21) and (22)).

$$x = 1 - \text{specificity} = 1 - \left[\frac{TN}{TN + FP} \right] \quad (21)$$

$$y = \text{sensitivity} = \frac{TP}{TP + FN} \quad (22)$$

later, the ROC's Area Under Curve (AUC) was calculated as the quantitative measure of implemented model performance. Furthermore, two other metrics of Overall Accuracy (OA, see Equation (23)) and Kappa Index (KI, see Equation (24)) were also calculated (Kanani-Sadat et al. 2019; Samanta et al. 2018).

$$\text{Overall Accuracy} = \frac{TP + TN}{TP + FP + TN + FN} \quad (23)$$

with a step of 0.01 for each threshold value ranging between 0 and 1, the OA value was repetitively calculated to acquire the best threshold value for labeling mangrove and non-mangrove areas. The threshold value given the optimum OA was selected (Kanani-Sadat et al. 2019; Shafapour Tehrany et al. 2019).

In the previous equations, TP (True Positive) and TN (True Negative) values are the numbers of points correctly classified as mangrove and non-mangrove points. FP (False Positive) denotes the number of non-mangrove points labeled as mangrove, and FN (False Negative) the number of mangrove points labeled as non-mangrove.

The KI was also considered for further assessment of the models' ability. A higher KI value shows that the model is more reliable (Khosravi et al. 2018).

$$KI = \frac{P_o - P_e}{1 - P_o} \quad (24)$$

in Equation (26), P_o is the correctly categorized rate of mangrove and non-mangrove points, and P_e represents the proportion of points in which the agreement would be expected due to chance (Janizadeh et al. 2019; Tehrany, Jones, and Shabani 2019). P_o and P_e were obtained using the following equations:

$$P_o = TP + TN \quad (25)$$

$$P_e = (TP + FN)(TP + FP) + (FP + TN)(FN + TN) \quad (26)$$

4. Results

This study considered the ten criteria (see Section 3.1) to generate a mangrove plantation suitability map in coastal areas of Hormozgan province, southern Iran. These criteria were then integrated within a GIS environment, and two methods of FDANP and AHP were applied to produce the final suitability maps, the results of which are provided in subsequent subsections.

4.1. Pearson correlation coefficient result

As already mentioned, the considered criteria might have possible interrelationships that could affect the final MCDM results (Kanani-Sadat et al. 2019). Accordingly, to consider the effect of these interdependencies, FDANP was implemented in this study. The Pearson correlation coefficient values were calculated to determine the possible interdependencies among criteria. As it is shown in Table 3, some of the considered criteria have a higher level of correlation with one another. The highest correlation values were observed between NDMI, NDVI, and NDSI. For instance, the Pearson correlation coefficient value between NDVI and NDSI is 0.83, which falls in the very strong correlation category, according to (Cao et al. 2020). On the other hand, some of the considered criteria had negligible and minor interdependencies, such as wind and NDVI and temperature and wind, respectively. This demonstrates the necessity of considering the interrelationships among criteria through DEMATEL to improve the final mangrove plantation suitability mapping.

4.2. Fuzzy-DEMATEL-ANP (FDANP)

As stated earlier, six steps should be conducted to calculate the final weight values based on the FDANP approach (see Section 3.1.2). After passing four steps, the defuzzified values of $\tilde{R}_i + \tilde{D}_j$ and $\tilde{R}_i - \tilde{D}_j$ were calculated to investigate the mutual impact of all criteria on each other. Based on Table 4, NDSI, NDMI, NDVI, temperature, and LULC with negative ($R_i - D_i$) values are influenced by other criteria and categorized into the group of “effects.” On the other side, Precipitation, DEM, Wind, Slope, and Solar radiation with positive ($R_i - D_i$) are assorted in the “causes” set. Considering ($R_i - D_i$) indicator, the factors can be ranked. Therefore, DEM has the most impact on other criteria while NDMI predominantly takes the influence from others. Also, the ($R_i + D_i$) parameter can be interpreted as the prominence of a criterion compared to others. Therefore, as shown in Table 4, temperature, precipitation, NDMI, and NDVI have

a critical position in the criteria network, and among all, the temperature is the most significant. This result logically makes sense since the temperature could affect the level of precipitation and, consequently, the moisture of the area and how vegetation changes depending on these criteria.

The α -cut total-relation matrix (Table 5) is obtained based on Equation 7 and 8. Afterward, the normalized α -cut total relation matrix (see supplementary material) is generated and multiplied by the relative importance pair-wise comparison matrix to generate the ANP weighted super-matrix (see Table 6). Finally, by limiting the weighted super-matrix powered to 7, the weighted super-matrix converged to a matrix with the same elements in each row, which were then used to calculate the final weights of all criteria (see Table 7).

Based on Table 7, NDVI and LULC were the most important criteria with weights values of 0.198 and 0.155, while the wind and solar radiation were the least important criteria with 0.029 and 0.030. Moreover, Figure 5 presents the mangrove plantation suitability map based on the FDANP approaches. Visual interpretation of the suitability map indicated that the highest suitability values were more proximate to existing mangrove ecosystems and near intertidal zones (i.e. area above or underwater level at low/high tides, respectively). Based on the validation step, the FDANP results obtained 95.76% and 94.68% specificity and sensitivity, respectively. Moreover, the OA and KI were

Table 4. Defuzzified values of importances and preferences of each criterion computed using fuzzy logic and DEMATEL.

Criteria	Deffuzified Values	
	$R_i + D_i$	$R_i - D_i$
Precipitation	1.492	0.486
Elevation	1.380	0.933
Wind	0.970	0.012
NDSI	1.116	-0.333
NDMI	1.476	-0.580
NDVI	1.468	-0.515
Slope	1.208	0.619
Temperature	1.535	-0.396
Solar radiation	1.342	0.102
LULC	1.334	-0.328

Table 3. Obtained Pearson correlation coefficient values between ten criteria considered to identify ecologically suitable locations for mangrove plantation.

	Precipitation	Elevation	Slope	Wind	Temperature	Solar radiation	NDVI	NDSI	NDMI	LULC
Precipitation	1.00	-0.10	-0.08	-0.15	-0.11	0.28	0.34	-0.34	0.39	-0.10
Elevation	-0.10	1.00	0.61	-0.02	0.30	0.04	-0.21	0.21	-0.36	0.18
Slope	-0.08	0.61	1.00	-0.04	0.30	0.06	-0.24	0.24	-0.36	0.21
Wind	-0.15	-0.02	-0.04	1.00	0.20	0.28	0.01	-0.01	-0.13	0.17
Temperature	-0.11	0.30	0.30	0.20	1.00	0.49	-0.45	0.45	-0.74	0.42
Solar radiation	0.28	0.04	0.06	0.28	0.49	1.00	0.09	-0.09	-0.01	0.22
NDVI	0.34	-0.21	-0.24	0.01	-0.45	0.09	1.00	-1.00	0.83	-0.04
NDSI	-0.34	0.21	0.24	-0.01	0.45	-0.09	-1.00	1.00	-0.83	0.04
NDMI	0.39	-0.36	-0.36	-0.13	-0.74	-0.01	0.83	-0.83	1.00	-0.27
LULC	-0.10	0.18	0.21	0.17	0.42	0.22	-0.04	0.04	-0.27	1.00

Table 5. The α -cut total-relation matrix obtained by filtering out the defuzzified total relation matrix.

	Precipitation	Elevation	Wind	NDSI	NDMI	NDVI	Slope	Temperature	Solar radiation	LULC
Precipitation	0.035	0.025	0.074	0.111	0.186	0.185	0.027	0.142	0.088	0.116
Elevation	0.120	0.022	0.100	0.102	0.126	0.158	0.105	0.127	0.169	0.127
Wind	0.047	0.000	0.021	0.051	0.061	0.077	0.020	0.113	0.026	0.056
NDSI	0.022	0.000	0.023	0.026	0.071	0.070	0.000	0.035	0.023	0.086
NDMI	0.025	0.000	0.024	0.067	0.035	0.112	0.000	0.054	0.024	0.070
NDVI	0.028	0.000	0.026	0.067	0.095	0.036	0.000	0.090	0.025	0.071
Slope	0.042	0.041	0.070	0.074	0.144	0.100	0.020	0.126	0.185	0.112
Temperature	0.102	0.020	0.063	0.042	0.086	0.086	0.021	0.042	0.031	0.076
Solar radiation	0.054	0.022	0.034	0.097	0.130	0.091	0.023	0.162	0.024	0.084
LULC	0.028	0.000	0.043	0.088	0.095	0.077	0.020	0.075	0.025	0.033

Table 6. Weighted supermatrix obtained by multiplying the normalized α -cut total relation matrix (Ts) by the relative importance pair-wise comparison matrix (W).

	Precipitation	Elevation	Wind	NDSI	NDMI	NDVI	Slope	Temperature	Solar radiation	LULC
Precipitation	0.035	0.051	0.377	0.056	0.375	0.047	0.054	0.430	0.536	0.118
Elevation	0.052	0.019	0.259	0.029	0.055	0.034	0.090	0.329	0.439	0.055
Wind	0.020	0.000	0.045	0.018	0.026	0.027	0.014	0.120	0.055	0.039
NDSI	0.126	0.000	0.389	0.072	0.796	0.098	0.000	0.390	0.323	0.242
NDMI	0.030	0.000	0.298	0.041	0.085	0.136	0.000	0.527	0.293	0.085
NDVI	0.257	0.000	0.362	0.307	0.432	0.083	0.000	0.819	0.338	0.162
Slope	0.023	0.045	0.230	0.027	0.053	0.022	0.022	0.276	0.811	0.061
Temperature	0.060	0.012	0.223	0.018	0.038	0.038	0.019	0.074	0.215	0.045
Solar radiation	0.013	0.010	0.047	0.027	0.036	0.021	0.008	0.056	0.033	0.029
LULC	0.057	0.000	0.264	0.182	0.395	0.159	0.084	0.466	0.207	0.068

Table 7. Final weights and the importance rank of each criterion using the Fuzzy-DEMATEL-ANP (FDANP) method.

	Precipitation	Elevation	Wind	NDSI	NDMI	NDVI	Slope	Temperature	Solar radiation	LULC
Weight of criteria	0.128	0.085	0.029	0.153	0.086	0.198	0.077	0.053	0.030	0.155
Rank	4	6	10	3	5	1	7	8	9	2

95.22% and 90.40%, respectively, representing the high potential of the FDANP approach.

4.3. Analytical hierarchy process

Table 8 provides the normalized pair-wise comparison matrix for the AHP method, which was then employed to calculate each criterion's final weight value (see Table 9). Accordingly, NDVI and NDSI were the most important criteria with weights values of 0.229 and 0.177, while wind and solar radiation were the least important criteria

with 0.027 and 0.024. Furthermore, Figure 6 presents the mangrove plantation suitability map based on the AHP approaches. Like the FDANP results, the visual interpretation of the suitability map indicated that the highest suitability values were closer to existing mangrove ecosystems and near intertidal zones. Based on the validation step, the AHP results achieved 92.56% and 90.91% specificity and sensitivity, respectively. Moreover, the OA and KI were 94.01% and 0.884, respectively, representing a satisfactory performance of the AHP approach.

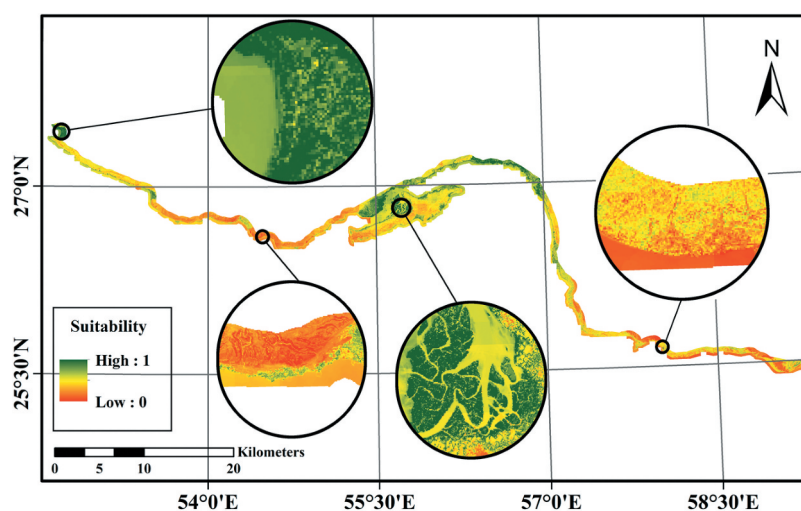
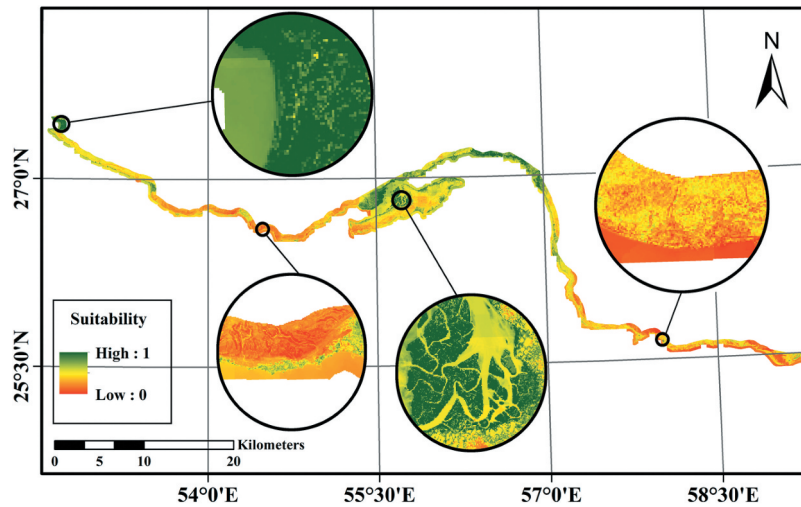
**Figure 5.** Final mangrove suitability map based on criteria weights obtained through the Fuzzy-DEMATEL-ANP (FDANP) method.

Table 8. The normalized average matrix of experts' pair-wise comparisons in the AHP method.

	Precipitation	Elevation	Wind	NDSI	NDMI	NDVI	Slope	Temperature	Solar radiation	LULC
Precipitation	0.098	0.125	0.143	0.083	0.160	0.058	0.111	0.121	0.154	0.156
Elevation	0.049	0.063	0.086	0.055	0.040	0.058	0.055	0.121	0.077	0.078
Wind	0.020	0.021	0.029	0.028	0.016	0.039	0.018	0.020	0.026	0.052
NDSI	0.196	0.188	0.171	0.166	0.320	0.117	0.166	0.162	0.128	0.156
NDMI	0.049	0.125	0.143	0.041	0.080	0.117	0.166	0.162	0.128	0.078
NDVI	0.392	0.250	0.171	0.331	0.160	0.233	0.276	0.162	0.154	0.156
Slope	0.049	0.063	0.086	0.055	0.027	0.047	0.055	0.081	0.103	0.078
Temperature	0.033	0.021	0.057	0.041	0.020	0.058	0.028	0.040	0.103	0.052
Solar radiation	0.016	0.021	0.029	0.033	0.016	0.039	0.014	0.010	0.026	0.039
LULC	0.098	0.125	0.086	0.166	0.160	0.233	0.111	0.121	0.103	0.156

Table 9. Final weights and the importance rank of each criterion using the AHP method.

	Precipitation	Elevation	Wind	NDSI	NDMI	NDVI	Slope	Temperature	Solar radiation	LULC
Weight of criteria	0.121	0.068	0.027	0.177	0.109	0.229	0.064	0.045	0.024	0.136
Rank	4	6	9	2	5	1	7	8	10	3

**Figure 6.** Final mangrove suitability map based on criteria weights obtained through the AHP method.

4.4. Comparisons

The final weight value of each criterion obtained by FDANP and AHP methods has changed based on Tables 7 and 9. The reason is that DEMATEL examines the interdependencies among criteria and considers their impact on weight calculation in the network. As expected, the ranking of the involved criteria did change in this study. For instance, “LULC” with a weight of 0.136 ranked 3 in the AHP method, but FDANP ranked this criterion as the second one with 0.155. Also, the order of “solar radiation” and “wind” has changed.

Moreover, the minor change in the final weight values slightly enhanced the suitability map (i.e. based on the statistical accuracy assessment) when incorporating interdependencies in the FDANP approach. The mangrove plantation suitability maps based on two approaches were provided in previous subsections. Statistical accuracy assessment (e.g. OA and KI) revealed that incorporating interdependencies between involved criteria through the FDANP improved the suitability map by about 1.21% and 1.98% in OA and KI, respectively. Furthermore, the

AUC of the ROC curves for both approaches was calculated (see Figure 7), manifesting the better performance of the FDANP method.

In a further step, for simplification of interpreting the generated mangrove plantation suitability maps, the final maps were classified into five classes, including “Very High”, “High”, “Medium”, “Low”, and “Very Low” using natural break method. The classified suitability map of FDANP is presented in Figure 8. Visual interpretation of the classified maps suggested a slight difference between the performances of both approaches. Additionally, the area of each class was computed to investigate the suitable area for mangrove plantations in Hormozgan Province (see Figure 9). The highest portion of the coastal area was identified as Moderate by the AHP approach, whereas the FDANP approach recognized Low as the dominant class. Likewise, based on the FDANP suitability map, 20.80% and 6.10% were classified as Very Low and Very High suitability. On the other hand, the AHP approach indicated 18.30% and 5.70% of the study area as Very Low and Very High suitability classes.

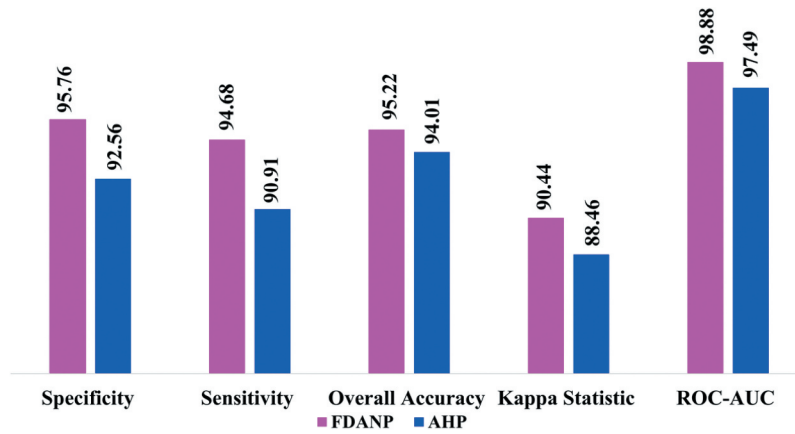


Figure 7. The statistical parameters for validation and comparison of Fuzzy-DEMATEL-ANP (FDANP) and AHP methods.

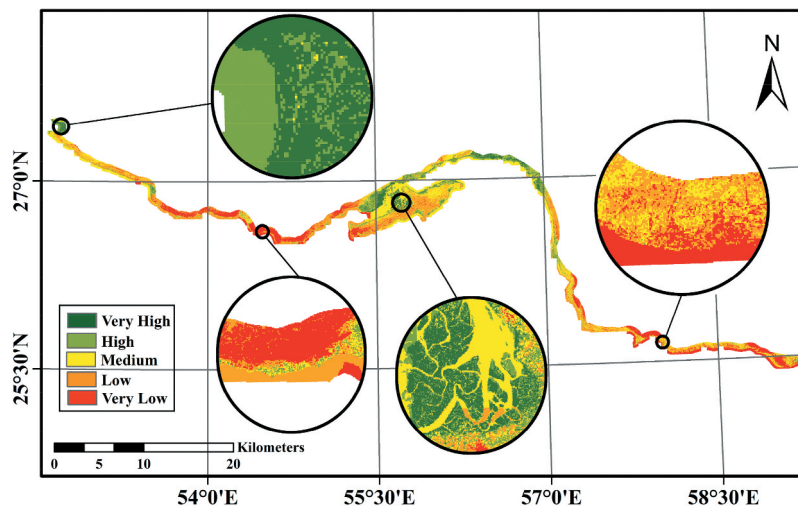


Figure 8. Classified mangrove suitability map generated based on the obtained criteria weights through the Fuzzy-DEMATEL-ANP (FDANP).

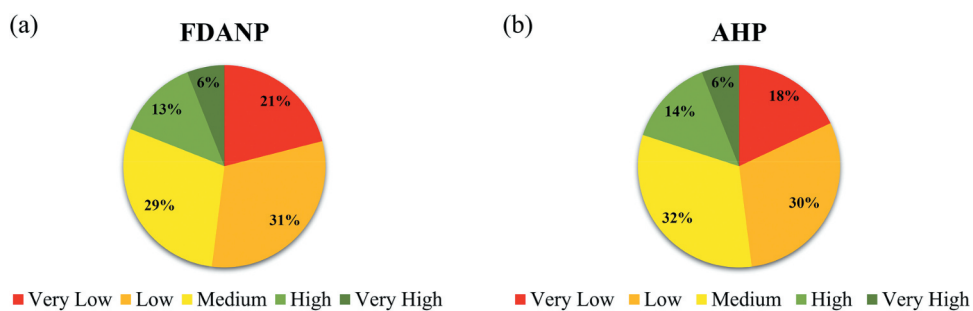


Figure 9. Individual class' suitability percentage based on generated mangrove suitability maps by (a) Fuzzy-DEMATEL-ANP (FDANP) and (b) AHP methods.

In the final step, the produced mangrove plantation suitability map based on FDANP was visually compared with high-resolution satellite imagery to explore the proposed method's applicability. In this regard, two regions with existing mangrove patches and one region with no mangrove patches were considered (see Figure 10). It is evident that the produced mangrove plantation suitability map had successfully delineated suitable locations for

mangrove plantation. This is according to the fact that regions with existing mangrove patches obtained relatively high suitability values. Moreover, the FDANP was capable of distinguishing ecologically unsuitable areas for mangrove plantation. For instance, in Figure 10 (upper circles), the zoomed area is covered by bare soil, and the outcrop covers with relatively higher distance to an intertidal zone that obtained low suitability values.

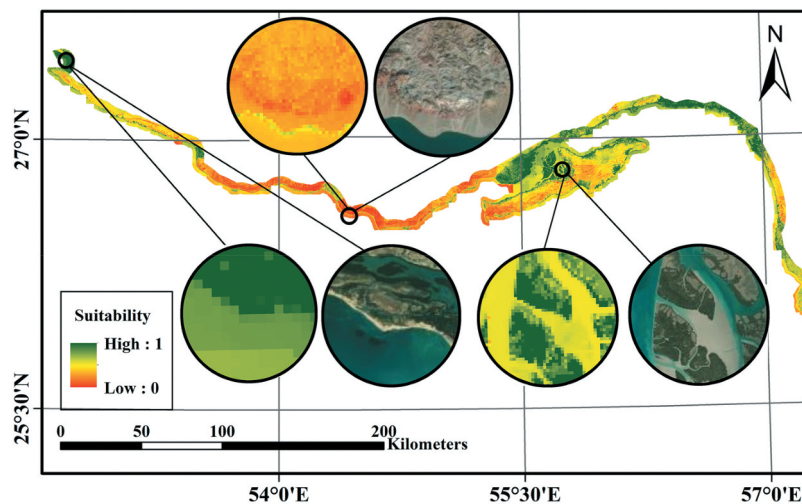


Figure 10. Comparison of generated mangrove suitability map and real-world mangroves.

5. Discussion

Studying mangroves has significant importance in conserving or restoring this threatened socio-ecological diversity since the rate of their disappearing is approximately one-third of the world's mangroves over the past 50 years (Baloloy et al. 2020). By disappearing this invaluable ecosystem, human is deprived of many socio-economic benefits, including flood and flow control, protecting the shoreline from storms and soil erosion, and carbon sink source (Amad et al. n.d; Maurya, Mahajan, and Chaube 2021; Zhuang et al. 2022). Furthermore, their importance for the surrounding environment has been recognized by various international organizations, and the restoration and conservation of mangrove ecosystems can support achieving several UN SDGs (e.g. Goals 14 and 15). In particular, the Global Mangrove Alliance partnership aligned a target (OceanAction14787, 2017) to increase mangrove habitat by 20% by 2030 as support to the UN SDG 14 (Alliance 2019). Accordingly, identifying suitable locations with accurate methods is mandatory to contribute toward prosperous mangrove plantations and lower the mortality of seedlings.

Consequently, the integration of RS and geospatial datasets and techniques make it possible to carry out such studies to support mangroves' conservation, restoration, and mainly plantation. However, few studies have employed RS and geospatial datasets to generate mangrove suitability maps through MDCM approaches. For instance, Chakraborty et al. (2019) applied the AHP method to generate the Future Mangrove Suitability Index (FMSI) using fourteen criteria and projected climatic data to investigate different future scenarios and stated that this study would strengthen future planning projects and research in the mangrove ecosystem management of the study area. In the study by Chakraborty et al. (2019), NDVI obtained a weight of 8 and ranked as the most

important criteria after soil salinity. In the current study, NDVI received a high weight and was ranked as the most important criterion. Moreover, comparing the weights of criteria indicates that the wind criterion has been recognized as the least important criterion in both studies. Moreover, Syahid et al. (2020) investigated Hydrodynamic, Geomorphological, and Climatic parameters combined with different climate models and the Representative Concentration Pathway (RCP) scenarios. In order to produce mangrove suitability maps, criteria were aggregated with both having the same weights and having different weights based on the AHP method. After identifying suitable locations for planting mangroves, this study analyzed the socio-economic parameters of the area and their influences on the land's suitability. According to criteria weights obtained by AHP, the geomorphological parameters had the highest weight (38% of the total weight), followed by the hydrodynamic parameters (32% of the total weight), and the Climatic parameter had the smallest weight (30% of the total weight). Geomorphological sub-parameters included elevation and slope, and the former was recognized as more important. In the current study, elevation also obtained a higher weight than slope, which is consistent with the previous studies (Syahid et al. 2020). In another study, (Jumawan and Macandog 2021) considered various criteria, including LULC, mangrove areas, soil types, slope, Philippine rivers, Philippine roads, Aster DEM, and boundary of Oriental Mindoro, for mangrove restoration in Oriental Mindoro, Philippines. The thematic maps of criteria were aggregated to obtain a suitability map using the AHP method and was classified into different suitability classes. Two thirds of municipalities in the province were recognized as suitable areas. Their results demonstrated the practicality of a GIS framework as a decision support technique for potential mangrove restoration initiatives. Despite the

efficiency of the above-mentioned works, they all implemented the traditional MCDM method named AHP, which is a simple method. AHP does not consider the interactions between criteria and uses crisp numbers to calculate the weight of criteria. In fact, environmental factors involved in the study may impact each other, and by considering them, a more accurate result can be achieved. Also, using fuzzy logic theory combined with the MCDM method can improve the reliability of results because decision-makers express their idea using verbal values instead of crisp numbers, which is more real. Unfortunately, there was no study in mangrove suitability analysis that considers these points.

Therefore, this study aimed to fill this gap, and a hybrid MCDM method named FDANP was compared to the traditional AHP method. These methods were combined with GIS and RS and geospatial datasets to map the potential area for restoration or plantation of mangroves along the southern coast of Iran. The results approve that the proposed method performed more efficiently in predicting potential mangrove areas. Moreover, the OA and KI of FDANP indicated that this method modeled mangrove suitability more precisely than the AHP method, which was in agreement with other relevant spatial modeling studies (Kanani-Sadat et al. 2019). The output of this study can help decision-makers and managers regarding future environmental and socio-economic plans to have a better insight into endangered areas. Using these maps can lead to minimizing the probability of planting mangroves' failure (Syahid et al. 2020).

Despite the efficiency of the current study, some limitations should be taken into account. For instance, a few parameters such as accurate population growth data and sea-level measurements should be included in further studies, unavailable throughout the study area due to data scarcity issues in developing countries like Iran. Moreover, a field-based survey should be done to obtain mangrove points in a dataset for the validation stage, which could allow a more robust accuracy assessment. Finally, future research can be directed toward Machine Learning (ML) approaches that do not require experts' knowledge and can decrease biases and vagueness.

6. Conclusions

Identifying suitable areas for mangrove forest plantation or restoration has become a necessary action that managers and decision-makers should consider. The rapid rate of mangrove ecosystem depletion is due to anthropogenic activities and natural drivers. The present study utilized a hybrid system to investigate and

map mangrove ecosystem suitability on the northern coast of the Persian Gulf and Oman Sea. It developed a hybrid MCDM approach that incorporated fuzzy logic, RS data, and GIS technology. The impact of ten criteria including precipitation, elevation, slope, wind, temperature, solar radiation, NDVI, NDSI, NDMI, and LULC was investigated on mangrove vegetation. These criteria were obtained from the GEE platform with a 100×100 m pixel size spatial resolution and used in a GIS environment to generate raster maps with the same pixel size. First, the DEMATEL approach was used to detect the impact of each criterion on others (inter-dependency), and as a result, there will be two groups of criteria called "Cause" and "Effect." Also, the fuzziness level of experts' judges has been managed by adopting fuzzy logic and merging it with the DEMATEL method. Fuzzy-DEMATEL results revealed that the DEM factor is an important criterion and significantly influences the other criteria. Then, the ANP approach was applied to calculate the weight of the criteria. NDVI has received the most weight value in mangrove ecosystem suitability mapping; the NDSI and LULC have the following ranks.

Moreover, solar radiation has the lowest impact on the resultant maps. To simplify the interpretation of obtained mangrove suitability maps, they are categorized into five classes. Furthermore, the assessment process was executed to certify the study's findings. Overlaying the obtained mangrove suitability maps with mangrove and non-mangrove points' dataset proves the verification and efficiency of the investigated hybrid approach. By comparing the implemented approaches, it can be concluded that FDANP with AUC = 98.8% outperformed AHP with AUC = 97.5%. Therefore, the proposed framework that investigates mangrove ecosystem suitability in a regional area can be helpful in spatial planning procedures. It provides decision-makers and managers with helpful information to deal with the degradation of this invaluable ecosystem by detecting endangered areas. Hence, by implementing appropriate strategies and increasing people's awareness in those regions, the level of loss can be reduced.

Acknowledgment

During this study, Roya Sahraei and Arsalan Ghorbanian were respectively funded by Erasmus + ICM programme for a 3-month and 5-month stay at Lund University, Lund, Sweden, and thank the European Union.

Disclosure statement

No potential conflict of interest was reported by the authors.

Notes on contributors

Roya Sahraei graduated from the University of Tehran in 2022 with an MSc degree in GIS. Also, she was a part of a team at Lund University working on mangrove mapping. Her research interests are Spatial Analysis, Environmental Monitoring and Management, Natural Hazards Modelling, Geomorphology, and Coastal Hazards. She intends to pursue her education as a PhD student.

Arsalan Ghorbanian received a BSc degree in geodesy and geomatics engineering in 2016 and an MSc degree in remote sensing in 2018 from the K. N. Toosi University of Technology, Tehran, Iran, where he is currently working toward a PhD degree in remote sensing. His research interests include LULC mapping, drought monitoring, geo-big data processing, wetland and mangrove studies, satellite image and video processing, and urban heat island studies. He has authored or co-authored 30 peer-reviewed publications in these fields. He has been a regular Reviewer in several international remote sensing journals and a Guest Editor for two Special Issues in the Remote Sensing journal. He also serves as an advisory board member of the Ecological Indicators journal. He has worked with different remote sensing datasets during his academic career, including multispectral, hyperspectral, synthetic aperture radar, and thermal infrared data. He was recognized as an excellent student during his BSc and ranked first during his MSc at the K. N. Toosi University of Technology. He was also selected as the Top Researcher in 2022 during his PhD at the K. N. Toosi University of Technology.

Yousef Kanani-Sadat is PhD Candidate in GIS at the School of Surveying and Geospatial Engineering, University of Tehran, Iran. He received his BSc degree in Surveying and Geomatics Engineering in 2012 and an MSc degree in GIS in 2015 from the University of Tehran. His current research interests include spatial modeling, GIS and remote sensing applications in hydrology, and spatial data mining.

Sadegh Jamali received the BSc degree in Surveying and Geomatics Engineering from the University of Tabriz, Iran, in 1998, the MSc degree in Geodesy from the University of Tehran, Iran, in 2000, and the PhD degree in Remote Sensing, from Lund University, Sweden, in 2014. In 2015, he was a Postdoctoral Fellow with the Department of Physical Geography and Ecosystem Sciences, Lund University, Sweden. In 2016, he joined the Department of Computer and Geospatial Sciences, Faculty of Engineering and Sustainable Development, Gävle University, Sweden, as a lecturer in Geomatics. Since 2017, he works as an Assistant Professor of Geomatics and Remote Sensing at the Department of Technology and Society, Faculty of Engineering (LTH), Lund University, Sweden. His research interests include land surface change analysis with a particular focus on developing methods for detecting changes and trends in time series of satellite data.

Saeid Homayouni is currently an associate professor of environmental remote sensing and geomatics at the Centre for Water, Land, and Environment of the Institut de la recherche Scientifique de Quebec. He holds a BS degree in Surveying and Geomatics Engineering, an MSc degree in remote sensing and GIS, and a PhD in signal and image. His research interests include the analysis of optical and radar Earth observations through AI, and ML approaches for urban and agro-environmental applications.

ORCID

Roya Sahraei  <http://orcid.org/0000-0003-0270-8208>
 Arsalan Ghorbanian  <http://orcid.org/0000-0001-8406-683X>
 Yousef Kanani-Sadat  <http://orcid.org/0000-0002-9215-5354>
 Sadegh Jamali  <http://orcid.org/0000-0002-0961-9497>
 Saeid Homayouni  <http://orcid.org/0000-0002-0214-5356>

Data availability statement

The remote sensing and geospatial datasets that support the findings of this study are publicly available through Google Earth Engine Data Catalog (<https://developers.google.com/earthengine/datasets>). The reference data are available from the first author (Roya Sahraei) upon a reasonable request.

References

- Al-Hanbali, A., K. Shibuta, B. Alsaideh, and Y. Tawara. 2021. "Analysis of the Land Suitability for Paddy Fields in Tanzania Using a GIS-Based Analytical Hierarchy Process." *Geo-Spatial Information Science* 25 (2): 1–17. doi:10.1080/10095020.2021.2004079.
- Ali, S. A., F. Parvin, Q. B. Pham, M. Vojtek, J. Vojteková, R. Costache, N. T. T. Linh, H. Q. Nguyen, A. Ahmad, and M. A. Ghorbani. 2020. "GIS-Based Comparative Assessment of Flood Susceptibility Mapping Using Hybrid Multi-Criteria Decision-Making Approach, Naïve Bayes Tree, Bivariate Statistics and Logistic Regression: A Case of Topľa Basin, Slovakia." *Ecological Indicators* 117: 106620. doi:10.1016/j.ecolind.2020.106620.
- Alireza, S. M., and J. Beglu Mansour. 2012. "Satellite Based Assessment of the Area and Changes in the Mangrove Ecosystem of the QESHM Island, Iran." *Journal Environmental Research Development* 7: 1052–1060.
- Alliance, G. M. 2019. "Taking Action to Increase Global Mangrove Habitat by 20 Percent by 2030: The Global Mangrove Alliance."
- Alpert, J. C. 2004. "Sub-Grid Scale Mountain Blocking at NCEP." In Proceedings of the 20th Conference on Weather and Forecasting and 16th Conference on Numerical Weather Prediction, Seattle, WA, USA.
- Amad, F. S., M. Z. M. Yunus, A. K. Abd Wahab, N. Ibrahim, and I. I. Mohamad. n.d. "Mapping the Mangrove Vulnerability Index Using Geographical Information System." *International Journal of Innovative Computing* 11 (1): 69–81. doi:10.11113/ijic.v11n1.309.
- Amani, M., A. Ghorbanian, S. A. Ahmadi, M. Kakooei, A. Moghimi, S. M. Mirmazloumi, S. H. Alizadeh Moghaddam, et al. 2020. "Google Earth Engine Cloud Computing Platform for Remote Sensing Big Data Applications: A Comprehensive Review." *IEEE Journal of Selected Topics in Applied Earth Observations and Remote Sensing* 13: 5326–5350. doi:10.1109/JSTARS.2020.3021052.
- Amiri, F. 2021. "Carbon Storage Potential of Avicennia Marina as Influenced by Soil Factors in National Park Nayband, South Coast of Iran." *Acta Ecologica Sinica* 41 (6): 566–574. doi:10.1016/j.chnaes.2021.06.005.
- Arabshiebani, R., Y. Kanani Sadat, and A. Abedini. 2016. "Land Suitability Assessment for Locating Industrial Parks: A Hybrid Multi Criteria Decision-making Approach Using Geographical Information System."

- Geographical Research* 54 (4): 446–460. doi:10.1111/1745-5871.12176.
- Ayçin, E., and S. Kayapinar Kaya. 2021. “Towards the Circular Economy: Analysis of Barriers to Implementation of Turkey’s Zero Waste Management Using the Fuzzy DEMATEL Method.” *Waste Management & Research* 39 (8): 1078–1089. doi:10.1177/0734242X20988781.
- Baloloy, A. B., A. C. Blanco, R. R. C. S. Ana, and K. Nadaoka. 2020. “Development and Application of a New Mangrove Vegetation Index (MVI) for Rapid and Accurate Mangrove Mapping.” *Isprs Journal of Photogrammetry and Remote Sensing* 166: 95–117. doi:10.1016/j.isprsjprs.2020.06.001.
- Bouamrane, A., O. Derdous, N. Dahri, S.E. Tachi, K. Boutebba, and M. T. Bouziane. 2020. “A Comparison of the Analytical Hierarchy Process and the Fuzzy Logic Approach for Flood Susceptibility Mapping in a Semi-Arid Ungauged Basin (Biskra Basin: Algeria).” *International Journal of River Basin Management* 20 (2): 1–11. doi:10.1080/15715124.2020.1830786.
- Buchhorn, M., M. Lesiv, N.E. Tsendbazar, M. Herold, L. Bertels, and B. Smets. 2020. “Copernicus Global Land Cover Layers—Collection 2.” *Remote Sensing* 12 (6): 1044. doi:10.3390/rs12061044.
- Büyüközkan, G., and G. Çifçi. 2012. “A Novel Hybrid MCDM Approach Based on Fuzzy DEMATEL, Fuzzy ANP and Fuzzy TOPSIS to Evaluate Green Suppliers.” *Expert Systems with Applications* 39 (3): 3000–3011. doi:10.1016/j.eswa.2011.08.162.
- Cabrera, J. S., and H. S. Lee. 2020. “Flood Risk Assessment for Davao Oriental in the Philippines Using Geographic Information System-Based Multi-Criteria Analysis and the Maximum Entropy Model.” *Journal of Flood Risk Management* 13 (2): e12607. doi:10.1111/jfr3.12607.
- Cao, Y., H. Jia, J. Xiong, W. Cheng, K. Li, Q. Pang, and Z. Yong. 2020. “Flash Flood Susceptibility Assessment Based on Geodetector, Certainty Factor, and Logistic Regression Analyses in Fujian Province, China.” *ISPRS International Journal of Geo-Information* 9 (12): 748. doi:10.3390/ijgi9120748.
- Chakraborty, S., S. Sahoo, D. Majumdar, S. Saha, and S. Roy. 2019. “Future Mangrove Suitability Assessment of Andaman to Strengthen Sustainable Development.” *Journal of Cleaner Production* 234: 597–614. doi:10.1016/j.jclepro.2019.06.257.
- Chen, V. Y. C., H.-P. Lien, C.-H. Liu, J. J. H. Liou, G.-H. Tzeng, and L.-S. Yang. 2011. “Fuzzy MCDM Approach for Selecting the Best Environment-Watershed Plan.” *Applied Soft Computing* 11 (1): 265–275. doi:10.1016/j.asoc.2009.11.017.
- Cormier-Salem, M. C., and J. Panfili. 2016. “Mangrove Reforestation: Greening or Grabbing Coastal Zones and Deltas? Case Studies in Senegal.” *African Journal of Aquatic Science* 41 (1): 89–98. doi:10.2989/16085914.2016.1146122.
- Dahdouh-Guebas, F. 2002. “The Use of Remote Sensing and GIS in the Sustainable Management of Tropical Coastal Ecosystems.” *Environment, Development and Sustainability* 4 (2): 93–112. doi:10.1023/A:1020887204285.
- Dano, U. L. 2021. “An AHP-Based Assessment of Flood Triggering Factors to Enhance Resiliency in Dammam, Saudi Arabia.” *GeoJournal* 87 (3): 1945–1960. doi:10.1007/s10708-020-10363-5.
- Das, S. 2020. “Flood Susceptibility Mapping of the Western Ghat Coastal Belt Using Multi-Source Geospatial Data and Analytical Hierarchy Process (AHP).” *Remote Sensing Applications: Society and Environment* 20: 100379. doi:10.1016/j.rsase.2020.100379.
- Datta, D., and S. Deb. 2012. “Analysis of Coastal Land Use/Land Cover Changes in the Indian Sunderbans Using Remotely Sensed Data.” *Geo-Spatial Information Science* 15 (4): 241–250. doi:10.1080/10095020.2012.714104.
- El Hussieny, S. A., K. H. Shaltout, and A. A. Alatar. 2021. “Carbon Sequestration Potential of *Avicennia Marina* (Forssk.) Vierh. and *Rhizophora Mucronata* Lam. Along the Western Red Sea Coast of Egypt.” *Rendiconti Lincei, Scienze Fisiche e Naturali* 32 (3): 599–607. doi:10.1007/s12210-021-01005-0.
- Falah, F., O. Rahmati, M. Rostami, E. Ahmadisharaf, I. N. Daliakopoulos, and H. Reza Pourghasemi. 2019. “Artificial Neural Networks for Flood Susceptibility Mapping in Data-Scarce Urban Areas.” In *Spatial Modeling in GIS and R for Earth and Environmental Sciences*, edited by G.-C. Fang and Z. Ayag, 323–336. London: Elsevier.
- Falatoonitoosi, E., S. Ahmed, and S. Sorooshian. 2014. “Expanded DEMATEL for Determining Cause and Effect Group in Bidirectional Relations.” *The Scientific World Journal* 2014: 1–7. doi:10.1155/2014/103846.
- Feizizadeh, B., M. Shadman Roodposhti, P. Jankowski, and T. Blaschke. 2014. “A GIS-Based Extended Fuzzy Multi-Criteria Evaluation for Landslide Susceptibility Mapping.” *Computers & Geosciences* 73: 208–221. doi:10.1016/j.cageo.2014.08.001.
- Feloni, E., I. Mousadis, and E. Baltas. 2020. “Flood Vulnerability Assessment Using a Gis-Based Multi-criteria Approach—The Case of Attica Region.” *Journal of Flood Risk Management* 13 (S1): e12563. doi:10.1111/jfr3.12563.
- Funk, C., P. Peterson, M. Landsfeld, D. Pedreros, J. Verdin, S. Shukla, G. Husak, et al. 2015. “The Climate Hazards Infrared Precipitation with Stations—A New Environmental Record for Monitoring Extremes.” *Scientific Data* 2 (1): 150066. doi:10.1038/sdata.2015.66.
- Gabus, A., and E. Fontela. 1973. “Perceptions of the World Problematique: Communication Procedure, Communicating with Those Bearing Collective Responsibility.”
- Ghorbanian, A., S. A. Ahmadi, M. Amani, A. Mohammadzadeh, and S. Jamali. 2022. “Application of Artificial Neural Networks for Mangrove Mapping Using Multi-Temporal and Multi-Source Remote Sensing Imagery.” *Water* 14 (2): 244. doi:10.3390/w14020244.
- Ghorbanian, A., S. Zaghian, R. M. Asiyabi, M. Amani, A. Mohammadzadeh, and S. Jamali. 2021. “Mangrove Ecosystem Mapping Using Sentinel-1 and Sentinel-2 Satellite Images and Random Forest Algorithm in Google Earth Engine.” *Remote Sensing* 13 (13): 2565. doi:10.3390/rs13132565.
- Ghorbanzadeh, O., B. Feizizadeh, and T. Blaschke. 2018. “Multi-Criteria Risk Evaluation by Integrating an Analytical Network Process Approach into GIS-Based Sensitivity and Uncertainty Analyses.” *Geomatics, Natural Hazards and Risk* 9 (1): 127–151. doi:10.1080/19475705.2017.1413012.
- Ghosh, M. K., L. Kumar, and C. Roy. 2016. “Mapping Long-Term Changes in Mangrove Species Composition and Distribution in the Sundarbans.” *Forests* 7 (12): 305. doi:10.3390/f7120305.
- Gigović, L., D. Pamučar, D. Lukić, and S. Marković. 2016. “GIS-Fuzzy DEMATEL MCDA Model for the Evaluation of the Sites for Ecotourism Development: A Case Study of

- “Dunavski Ključ” Region, Serbia.” *Land Use Policy* 58: 348–365. doi:10.1016/j.landusepol.2016.07.030.
- Giri, C. 2021. “Recent Advancement in Mangrove Forests Mapping and Monitoring of the World Using Earth Observation Satellite Data.” *Remote Sensing* 13 (4): 563. Multidisciplinary Digital Publishing Institute. doi:10.3390/rs13040563.
- Gorelick, N., M. Hancher, M. Dixon, S. Ilyushchenko, D. Thau, and R. Moore. 2017. “Google Earth Engine: Planetary-Scale Geospatial Analysis for Everyone.” *Remote Sensing of Environment* 202: 18–27. doi:10.1016/j.rse.2017.06.031.
- Hu, W., Y. Wang, D. Zhang, W. Yu, G. Chen, T. Xie, Z. Liu, et al. 2020. “Mapping the Potential of Mangrove Forest Restoration Based on Species Distribution Models: A Case Study in China.” *The Science of the Total Environment* 748: 142321. doi:10.1016/j.scitotenv.2020.142321.
- Janizadeh, S., M. Avand, A. Jaafari, T. V. Phong, M. Bayat, E. Ahmadisharaf, I. Prakash, B. T. Pham, and S. Lee. 2019. “Prediction Success of Machine Learning Methods for Flash Flood Susceptibility Mapping in the Tafresh Watershed, Iran.” *Sustainability* 11 (19): 5426. doi:10.3390/su11195426.
- Jarvis, A., H. Isaak Reuter, A. Nelson, and E. Guevara. 2008. “Hole-Filled SRTM for the Globe Version 4.” Available from the CGIAR-CSI SRTM 90m Database ([Http://Srtm.Csi.Cgiar.Org](http://Srtm.Csi.Cgiar.Org)) 15 (25–54): 5.
- Jassbi, J., F. Mohamadnejad, and H. Nasrollahzadeh. 2011. “A Fuzzy DEMATEL Framework for Modeling Cause and Effect Relationships of Strategy Map.” *Expert Systems with Applications* 38 (5): 5967–5973. doi:10.1016/j.eswa.2010.11.026.
- Jayanthi, M., S. Thirumurthy, G. Nagaraj, M. Muralidhar, and P. Ravichandran. 2018. “Spatial and Temporal Changes in Mangrove Cover Across the Protected and Unprotected Forests of India.” *Estuarine, Coastal and Shelf Science* 213: 81–91. doi:10.1016/j.ecss.2018.08.016.
- Jumawan, J. H., and D. M. Macandog. 2021. “GIS Weighted Suitability Analysis as Decision Support Tool for Mangrove Rehabilitation in Oriental Mindoro, Philippines.” *Journal of Ecosystem Science and Eco-Governance Vol 3* (1): 1–13.
- Kamal, M., S. Phinn, and K. Johansen. 2015. “Object-Based Approach for Multi-Scale Mangrove Composition Mapping Using Multi-Resolution Image Datasets.” *Remote Sensing* 7 (4): 4753–4783. doi:10.3390/rs70404753.
- Kanani-Sadat, Y., R. Arabsheibani, F. Karimipour, and M. Nasser. 2019. “A New Approach to Flood Susceptibility Assessment in Data-Scarce and Ungauged Regions Based on GIS-Based Hybrid Multi Criteria Decision-Making Method.” *Journal of Hydrology* 572: 17–31. doi:10.1016/j.jhydrol.2019.02.034.
- Khosravi, K., B. Thai Pham, K. Chapi, A. Shirzadi, H. Shahabi, I. Revhaug, I. Prakash, and D. T. Bui. 2018. “A Comparative Assessment of Decision Trees Algorithms for Flash Flood Susceptibility Modeling at Haraz Watershed, Northern Iran.” *The Science of the Total Environment* 627: 744–755. doi:10.1016/j.scitotenv.2018.01.266.
- Mafi-Gholami, D., A. Jaafari, E. K. Zenner, A. Nouri Kamari, and D. Tien Bui. 2020. “Spatial Modeling of Exposure of Mangrove Ecosystems to Multiple Environmental Hazards.” *The Science of the Total Environment* 740: 140167. doi:10.1016/j.scitotenv.2020.140167.
- Mahmoud, S. H., and T. Y. Gan. 2018. “Multi-Criteria Approach to Develop Flood Susceptibility Maps in Arid Regions of Middle East.” *Journal of Cleaner Production* 196: 216–229. doi:10.1016/j.jclepro.2018.06.047.
- Mark, H., A. Dencer-Brown, K. Diele, K. Kathiresan, I. Nagelkerken, and C. Wanjiru. 2017. “Mangroves and People: Local Ecosystem Services in a Changing Climate BT - Mangrove Ecosystems: A Global Biogeographic Perspective: Structure, Function, and Services.” In edited by V. H. Rivera-Monroy, S. Y. Lee, E. Kristensen, and R. R. Twilley, 245–274. Cham: Springer International Publishing. doi:10.1007/978-3-319-62206-4_8.
- Matani, O. P. M., M. I. Aipassa, S. Hardwinarto, and M. Sumaryono. 2021. “West Papua Mangrove Management Strategy (Case Study of Oransbari Mangrove Area in South Manokwari Regency).”
- Maurya, K., S. Mahajan, and N. Chaube. 2021. “Remote Sensing Techniques: Mapping and Monitoring of Mangrove Ecosystem—A Review.” *Complex & Intelligent Systems* 7 (6): 2797–2818. doi:10.1007/s40747-021-00457-z.
- Mavi, R. K., and C. Standing. 2018. “Critical Success Factors of Sustainable Project Management in Construction: A Fuzzy DEMATEL-ANP Approach.” *Journal of Cleaner Production* 194: 751–765. doi:10.1016/j.jclepro.2018.05.120.
- Melo, R. H., C. Kusmana, E. Eriyatno, and D. R. Nurrochmat. 2020. “Mangrove Forest Management Based on Multi Dimension Scalling (RAP-Mforest) in Kwandang Sub-District, North Gorontalo District, Indonesia.” *Biodiversitas Journal of Biological Diversity* 21 (4). doi:10.13057/biodiv/d210411.
- “OceanAction14787.” 2017. <https://oceanconference.un.org/commitments/?id=14787>
- Omar, H., M. A. Mismam, and S. Musa. 2019. “GIS and Remote Sensing for Mangroves Mapping and Monitoring.” *Geographic Information Systems and Science* 101: 101–115. doi:10.5772/intechopen.81955.
- Omo-Irabor, O. O., S. B. Olobaniyi, J. Akunna, V. Venus, J. M. Maina, and C. Paradzayi. 2011. “Mangrove Vulnerability Modelling in Parts of Western Niger Delta, Nigeria Using Satellite Images, GIS Techniques and Spatial Multi-Criteria Analysis (SMCA).” *Environmental Monitoring and Assessment* 178 (1): 39–51. doi:10.1007/s10661-010-1669-z.
- Osei Darko, P., M. Kalacska, J. P. Arroyo-Mora, and M. E. Fagan. 2021. “Spectral Complexity of Hyperspectral Images: A New Approach for Mangrove Classification.” *Remote Sensing* 13 (13): 2604. doi:10.3390/rs13132604.
- Pattanaik, C., and S. N. Prasad. 2011. “Assessment of Aquaculture Impact on Mangroves of Mahanadi Delta (Orissa), East Coast of India Using Remote Sensing and GIS.” *Ocean & Coastal Management* 54 (11): 789–795. doi:10.1016/j.ocecoaman.2011.07.013.
- Phochanikorn, P., and C. Tan. 2019. “An Integrated Multi-Criteria Decision-Making Model Based on Prospect Theory for Green Supplier Selection Under Uncertain Environment: A Case Study of the Thailand Palm Oil Products Industry.” *Sustainability* 11 (7): 1872. doi:https://doi.org/10.3390/su11071872.
- Ravanelli, R., A. Nascetti, R. V. Cirigliano, C. Di Rico, G. Leuzzi, P. Monti, and M. Crespi. 2018. “Monitoring the Impact of Land Cover Change on Surface Urban Heat Island Through Google Earth Engine: Proposal of a Global Methodology, First Applications and Problems.” *Remote Sensing* 10 (9): 1488. doi:https://doi.org/10.3390/rs10091488.

- Richards, D. R., and D. A. Friess. 2016. "Rates and Drivers of Mangrove Deforestation in Southeast Asia, 2000–2012." *Proceedings of the National Academy of Sciences* 113 (2): 344–349. doi:10.1073/pnas.1510272113.
- Saaty, T. L. 1977. "A Scaling Method for Priorities in Hierarchical Structures." *Journal of Mathematical Psychology* 15 (3): 234–281. doi:10.1016/0022-2496(77)90033-5.
- Saaty, T. L. 1980. *The Analytic Hierarchy Process. Planning, Priority Setting, Resource Allocation*. New York, NY, USA: McGraw-Hill.
- Saaty, T. L. 1996. *Decision Making with Dependence and Feedback: The Analytic Network Process*. Vol. 4922. Pittsburgh, PA, USA: RWS publications Pittsburgh.
- Saha, S., S. Moorthi, W. Xingren, J. Wang, S. Nadiga, P. Tripp, D. Behringer, H.-Y.C. Yu-Tai Hou, and M. Iredell. 2011. "NCEP Climate Forecast System Version 2 (CFSv2) 6-Hourly Products." *Research Data Archive at the National Center for Atmospheric Research, Computational and Information Systems Laboratory* 10: D61C1TXF.
- Sakti, A. D., A. Irwansyah Fauzi, F. Niwan Wilwatikta, Y. Sepwanto Rajagukguk, S. Adhitya Sudhana, L. Fajri Yayusman, L. Nurlaila Syahid, et al. 2020. "Multi-Source Remote Sensing Data Product Analysis: Investigating Anthropogenic and Naturogenic Impacts on Mangroves in Southeast Asia." *Remote Sensing* 12 (17): 2720. doi:10.3390/rs12172720.
- Samanta, R. K., G. S. Bhunia, P. K. Shit, and H. R. Pourghasemi. 2018. "Flood Susceptibility Mapping Using Geospatial Frequency Ratio Technique: A Case Study of Subarnarekha River Basin, India." *Modeling Earth Systems and Environment* 4 (1): 395–408. doi:10.1007/s40808-018-0427-z.
- Sangaiah, A. K., J. Gopal, A. Basu, and P. R. Subramaniam. 2017. "An Integrated Fuzzy DEMATEL, TOPSIS, and ELECTRE Approach for Evaluating Knowledge Transfer Effectiveness with Reference to GSD Project Outcome." *Neural Computing & Applications* 28 (1): 111–123. doi:10.1007/s00521-015-2040-7.
- Savari, M., H. E. Damaneh, and H. E. Damaneh. 2022. "Factors Involved in the Degradation of Mangrove Forests in Iran: A Mixed Study for the Management of This Ecosystem." *Journal for Nature Conservation* 66: 126153. doi:10.1016/j.jnc.2022.126153.
- Shabani, M., Z. Masoumi, and A. Rezaei. 2022. "Assessment of Groundwater Potential Using Multi-Criteria Decision Analysis and Geoelectrical Surveying." *Geo-Spatial Information Science* 25 (4): 1–19. doi:10.1080/10095020.2022.2069052.
- Shafapour Tehrany, M., L. Kumar, M. Neamah Jebur, and F. Shabani. 2019. "Evaluating the Application of the Statistical Index Method in Flood Susceptibility Mapping and Its Comparison with Frequency Ratio and Logistic Regression Methods." *Geomatics, Natural Hazards and Risk* 10 (1): 79–101. doi:10.1080/19475705.2018.1506509.
- Soner, O. 2021. "Application of Fuzzy DEMATEL Method for Analysing of Accidents in Enclosed Spaces Onboard Ships." *Ocean Engineering* 220: 108507. doi:10.1016/j.oceaneng.2020.108507.
- Sorourkhah, A., and S. A. Edalatpanah. 2022. "Using a Combination of Matrix Approach to Robustness Analysis (MARA) and Fuzzy DEMATEL-Based ANP (FDANP) to Choose the Best Decision." *International Journal of Mathematical, Engineering and Management Sciences* 7 (1): 68. doi:10.33889/IJMEMS.2022.7.1.005.
- Sushobhan, M., U. Chatterjee, B. Koley, G. Sankar Bhunia, P. Kumar Shit, U. Chatterjee, and K. C. Lalmalsawmzauva. 2022. "Object-Based Mapping and Modelling of Sundarban Mangrove Forests in India BT - Anthropogeomorphology: A Geospatial Technology Based Approach." In edited by G. S. Bhunia and P. K. Shit, 411–426. Cham: Springer International Publishing. doi:10.1007/978-3-030-77572-8_21.
- Swamy, L., E. Drazen, W. R. Johnson, and J. J. Bukoski. 2018. "The Future of Tropical Forests Under the United Nations Sustainable Development Goals." *Journal of Sustainable Forestry* 37 (2): 221–256. doi:10.1080/10549811.2017.1416477.
- Syahid, L. N., A. D. Sakti, R. Virtriana, K. Wikantika, W. Windupranata, S. Tsuyuki, R. E. Caraka, and R. Pribadi. 2020. "Determining Optimal Location for Mangrove Planting Using Remote Sensing and Climate Model Projection in Southeast Asia." *Remote Sensing* 12 (22): 3734. doi:10.3390/rs12223734.
- Tehrany, M. S., S. Jones, and F. Shabani. 2019. "Identifying the Essential Flood Conditioning Factors for Flood Prone Area Mapping Using Machine Learning Techniques." *Catena* 175: 174–192. doi:10.1016/j.catena.2018.12.011.
- Torre, D. M. G. D., J. Gao, C. Macinnis-Ng, and Y. Shi. 2021. "Phenology-Based Delineation of Irrigated and Rain-Fed Paddy Fields with Sentinel-2 Imagery in Google Earth Engine." *Geo-Spatial Information Science* 24 (4): 695–710. doi:10.1080/10095020.2021.1984183.
- Veettil, B. K., D. D. Van, N. X. Quang, and P. N. Hoai. 2020. "Spatiotemporal Dynamics of Mangrove Forests in the Andaman and Nicobar Islands (India)." *Regional Studies in Marine Science* 39: 101455. doi:10.1016/j.rsma.2020.101455.
- Vinodh, S., T. S. Sai Balagi, and A. Patil. 2016. "A Hybrid MCDM Approach for Agile Concept Selection Using Fuzzy DEMATEL, Fuzzy ANP and Fuzzy TOPSIS." *International Journal of Advanced Manufacturing Technology* 83 (9): 1979–1987. doi:10.1007/s00170-015-7718-6.
- Wang, Y., H. Hong, W. Chen, S. Li, D. Pamučar, L. Gigović, S. Drobnjak, D. Tien Bui, and H. Duan. 2019. "A Hybrid GIS Multi-Criteria Decision-Making Method for Flood Susceptibility Mapping at Shangyou, China." *Remote Sensing* 11 (1): 62. doi:10.3390/rs11010062.
- Woodroffe, C. D. 1990. "The Impact of Sea-Level Rise on Mangrove Shorelines." *Progress in Physical Geography: Earth and Environment* 14 (4): 483–520. doi:10.1177/030913339001400404.
- Zadeh, L. A., G. J. Klir, and B. Yuan. 1996. "Fuzzy Sets, Fuzzy Logic, and Fuzzy Systems: Selected Papers." *Advances in Fuzzy Systems: Applications and Theory*. World Scientific. <https://books.google.com/books?id=wu0dMiIHwJkC>
- Zhuang, Q., Z. Shao, D. Li, X. Huang, O. Altan, W. Shixin, and Y. Li. 2022, September. "Isolating the Direct and Indirect Impacts of Urbanization on Vegetation Carbon Sequestration Capacity in a Large Oasis City: Evidence from Urumqi, China." *Geo-Spatial Information Science* 1–13. doi:10.1080/10095020.2022.2118624.